NASA CR-159445

159445

ELEVATED TEMPERATURE PROPERTIES OF BORON/ALUMINUM COMPOSITES

by

P.G. SULLIVAN

NEVADA ENGINEERING & TECHNOLOGY CORP.
2225 EAST 28th STREET, BLDG. 511
LONG BEACH, CA 90806

prepared for

NATIONAL AERONAUTICS AND SPACE ADMINISTRATION

NASA Lewis Research Center

Contract NAS 3-20079

D.L. McDANELS, Project Manager

TABLE OF CONTENTS

LIST OF TABLES

LIST OF FIGURES

LIST OF APPENDICES

FOREWORD

This final technical report summarizes the work performed during the period 26 January 1976 through 26 June 1977 under Contract No. NAS3-20079 ("Elevated Temperature Properties of Boron-Aluminum Composites") for NASA-Lewis Research Center. The NASA-Lewis Project Manager was D.L. McDanels (106-1). The NETCO Program Manager was L.W. Davis, the Principal Investigator was P.G. Sullivan. Other personnel contributing to the program were J.F. Dolowy and B.A. Webb of DWA Composite Specialties and C.B. Gilpin of California State University - Long Beach.

SUMMARY

The primary objective of this program was the establishment of the high temperature properties of boron/aluminum composites fabricated by an air diffusion bonding technique utilizing vacuum-bonded monolayer tape. Conventional boron/aluminum composites are fabricated by an all-vacuum diffusion bonding process.

Secondary objectives included:

1. The determination of the effect of two different diameters of B/W fiber on mechanical properties and
2. The determination of the effect of titanium cladding and interleaving on mechanical properties.

Seventeen different combinations of matrix alloy, reinforcement diameter, reinforcement volume percent, angle-ply and "matrix enhancement" (i.e., titanium cladding and interleaves) were fabricated, inspected, and tested.

It was demonstrated that, with proper selection of fabrication pressure, temperature and time for each combination, good to excellent mechanical properties could be obtained for air-bonded boron/aluminum composites and that these properties did not decrease significantly up to test temperature of at least 260°C (500°F). Composites made with 8 mil B/W fiber showed a much greater longitudinal strength dependence on volume percent fiber than did composites made with 5.6 mil fiber. In both types of composite the addition of titanium caused difficulties in composite bonding and yielded composites with reduced strength.

INTRODUCTION

Although there exists considerable property information for vacuum, or inert atmosphere, diffusion bonded B/Al at room and elevated temperatures, little is known about the properties of B/Al fabricated by diffusion bonding in air. Such information is necessary if these materials are to be utilized in advanced turbine engine applications having higher operating efficiencies and operational temperatures. Establishing these properties will provide a sound technical base for determining the potential of air-bonded B/Al composites for use as fan and compressor blade materials.

Air diffusion bonding of B/Al can result in important cost savings since time at temperature is shorter, thus reducing man-power and equipment usage, and since fewer and less costly steps are required in part fabrication. In the past, most B/Al composites have been fabricated in vacuum in order to retard the formation of aluminum diboride (AlB_2) on the boron filaments. Klein, Metcalfe and Gulden (1) have extensively studied B/Al composite degradation accompanying elevated temperature exposures and concluded that degradation resulted from AlB_2 formation on the boron filaments. Reference 1 also reported the following:

- Removal of the AlB_2 from filament surfaces restores the original filament strength.
- Aluminum oxide originally at the Al/B interface may control the kinetics of AlB_2 formation and growth.
- Breakdown of the Al_2O_3 film by spheroidization and fracture permits the initial formation of AlB_2.

- Up to about an hour at 940°F is required before room temperature tensile strength and fracture strain are degraded by AlB_2 formation.
- Exposure at 700°F for 2300 hours does not result in AlB_2 formation, and more than 10,000 hours might be required at 700°F to reduce the composite tensile strength by one-half.
- Exposure in air at temperatures and times too low to produce AlB_2 cause property degradation if the B filaments are not protected from the air by an adequate matrix-matrix bond.
- Cyclic heating exposure of 6061 Al/45 v/o B composites to 800°-940°F had essentially the same effects on mechanical properties as continuous exposures for equivalent times.

Although filament-matrix reactions, filament properties, and composite properties have been evaluated (1-17), the quantitative influence of air exposure during fabrication and testing was not evaluated in these reports.

PROGRAM OBJECTIVES

The overall objective of this program was the establishment of room temperature and elevated temperature mechanical properties of air diffusion bonded boron/aluminum composites. Secondary objectives included establishment of bonding parameters as these were influenced by fiber diameter, fiber volume percent, angle-ply, matrix alloy and "matrix enhancement" (i.e., titanium cladding and interleaving).

The purpose of this program was to determine whether B/Al composites which are air diffusion bonded yield mechanical properties which equal or exceed those of vacuum diffusion bonded composites at room temperature and elevated temperatures.

PROGRAM APPROACH

The program was carried out in four tasks. A general flow diagram is presented in Figure I. Task I consisted of panel fabrication qualification and test panel fabrication. Five different combinations were selected to be air diffusion bonded for qualification. These were Combinations 1, 5, 8, 13 and 14 (see Table I-1). In addition, Combinations 5 and 6 were fabricated by vacuum diffusion bonding for use as controls. These panels were non-destructively and destructively inspected to establish fabrication qualification. Task I also consisted of fabricating seventeen different Combinations of fiber diameter, fiber volume percent, angle ply, matrix alloy and matrix enhancement. Task II consisted of 1) non-destructive inspection to establish panel integrity and 2) mechanical property characterization at room temperature and elevated temperatures of the material fabricated in Task I. Task III consisted of delivery of four composite panels to NASA-Lewis for further evaluation. Task IV consisted of monthly, quarterly and final reports.

DISCUSSION

In the past the trend in B/Al composites has been to maximize composite strength by the use of the highest strength matrix, usually 2024 Al or 6061 Al. Unfortunately, this has produced composites with less than desirable impact strength. Since one of the very real hazards encountered by aircraft engine fan blades made of B/Al is foreign-object-damage (FOD) caused by impacts with birds, the toughness and ductility of the matrix could be more important than ultimate strength. Two matrix materials were chosen for investigation in this program. 1100 Al was chosen as the primary matrix material since other NASA programs had already demonstrated superior impact properties from 1100 Al matrix composites. Another advantage of 1100 Al is its relatively high solidus temperature (>645°C (>1190°F)) and its decreased reactivity with boron fibers relative to 6061 Al. 2024 Al was chosen as the secondary matrix material for investigation because it has superior elevated temperature properties relative to 6061 Al and higher tensile properties than 1100 Al at temperatures up to 260°C (500°F).

Two diameters of B/W fibers were chosen for use in this program: 5.6 mil and 8 mil. These were chosen over 4.0 mil fiber since the larger surface-to-volume ratio of the larger fibers helps to improve the impact strength of the composites by providing a larger filament-matrix interface area for debonding on impact. The larger amount of matrix surrounding each fiber is also less constrained allowing the inherent ductility of the matrix to absorb more energy on impact.

Volume percent of fiber was varied from 50 v/o to 60 v/o in order to assess the influence of fiber volume percent on ultimate strength properties and fabrication parameters.

Matrix enhancement was added to some of the combinations in the form of ∿.08 mm (3 mil) Ti-6Al-4V foil on both surfaces and at the midplane of the composite.

All composites consisted of 8 layers of B/Al; to some of these composites Ti-6Al-4V was added on the surfaces and between the 4th and 5th B/Al layers (midplane) as an additional method of improving impact resistance. Table I-1 lists the combinations of the seventeen combinations investigated. Eight of the combinations were unidirectional layups and nine were balanced $\pm$ 15° layups.

Task I - Qualification and Fabrication

The purpose of this task was to qualify the air bonding fabrication process (Phase I) and fabrication of all combinations required for test in Task II (Phase II) and deliverables in Task III (Phase III).

Phase I. Fabrication Qualification. The purpose of this phase was to qualify the fabricator of the air bonded test panels. DWA Composite Specialties fabricated all the B/Al composites used in this program.

Fabrication. All of the B/Al made in this program was made by a two step process. Fully dense vacuum diffusion bonded monotape,

laid-up to the proper volume percent fiber, was subsequently air diffusion bonded into 8 ply panels. The monolayer was vacuum diffusion bonded using a nominal 538°C/30 minutes/20 MPa (1000°F/30 minutes/3 ksi) bonding cycle. The 8-layer panels were fabricated in air using a nominal 565°C/15 minutes/28 MPa (1050°F/15 minutes/4 ksi) bond cycle. The aluminum was abraded and cleaned with a hydrofluoric-nitric acid solution and rinsed before layup and bonding. The titanium was also abraded and cleaned before layup and bonding.

General Procedure for Qualification. The dimensions of the qualification panels were 102 mm (4 in.) x 152 mm (6 in.) x 8 layer. After fabrication the panels were inspected by ultrasonic C-Scan. A complete description of the method is given in Appendix A. The C-Scans were examined for bonding non-uniformity and misaligned fibers. Longitudinal and transverse tensile specimens (see Appendix B for test specimen geometry) were machined from the panels and tested to establish bonding qualification.

Combinations 1, 5, 8, 13 and 14 were used to qualify the air bonding technique. The first set of panels yielded satisfactory test results for combinations 8, 13 and 14. The results for combination 5 were low but since combination 13 was the same composition it was decided not to remake this panel. Combinations 1, 2 and 3 were remade. The second iteration of combinations 1 and 2 yielded satisfactory results. Combination 3 was subsequently made two more times in an attempt to retain high longitudinal

strength while producing good transverse strength. The third remake was judged satisfactory. Table I-2 shows the average results and comparisons of all the qualification tests.

It was found for 1100 Al that the bonding parameters, within limits, affected the bond quality less than cleanliness and proper preparation of the aluminum surfaces to be bonded. All of the air bonded material was bonded at 565°C/15 minutes/28 MPa pressure (1050°F/15 minutes/4 ksi). It was the soundness of the monolayer bond, produced with a bond cycle in vacuum of 538°C/30 minutes/20 MPa pressure (1000°F/30 minutes/3 ksi), and the subsequent surface preparation which were critical in achieving a well bonded composite.

When bonding is done in air, it is appreciably more difficult to obtain a sound bond with 1100 Al than with either 2024 Al or 6061 Al. Air diffusion bonding is performed between the solidus and liquidus temperature but in 1100 Al (essentially pure Al) there is no spread between solidus and liquidus and bonding must take place below the solidus temperature.

Phase II. Production of Test Panels. The purpose of this task was production of the B/Al material required in Task II. The seventeen combinations to be tested were made in the following configurations using the method qualified in Phase I of Task I. At least two panels were made for each combination: one panel 203 mm x 609 mm x 8 layers (8 in x 24 in x 8 layers), with the fibers longitudinal

in the 609 mm (24 in) direction, and one panel 203 mm x 229 mm x 8 layers (8 in x 9 in x 8 layers), with the fibers longitudinal in the 203 mm (8 in) direction. All longitudinal specimens were machined from the large panel and all transverse specimens were machined from the small panel.

Task II - Property Characterization

The purpose of this task was characterization of the B/Al panels produced in Task I-Phase II. The characterization included room and elevated temperature longitudinal and transverse tensile properties, longitudinal room and elevated temperature shear properties, room temperature and elevated temperature longitudinal fatigue properties and determination of longitudinal and transverse thermal coefficient of expansion up to 371°C (700°F).

General Procedure. The following procedure was followed for all material tested:

1. C-Scan. After receipt of the test panels, ultrasonic C-Scan was performed to identify any non-bonded regions or non-aligned fibers. Appendix A describes the C-Scan technique.
2. Specimen Layout and Machining. Although a master specimen layout was used for most panels, if the C-Scan of a panel showed suspect regions the specimen layout was modified to avoid those regions. Where this was impractical, another panel was made. In the detailed discussion of test results, remade panels will be identified. Appendix B details master

panel specimen layouts and specimen geometries for each type of test. The specimen dimensions are tabulated in Table II-1 for reference. All specimens were 8 layers thick.

All specimens were machined from test panels using a 1 mm thick fixed position diamond cut-off wheel vertically mounted on a floor pedestal milling machine. This produced a specimen edge which was smooth enough to require no finish grinding before test. Appendix C details all testing procedures.

Results - All Combinations Except 15, 16 and 17. A complete tabulation of all test results is in Appendix D. The organization of Tables and Figures pertinent to this section and in Appendix D will follow this convention:

1. All tables having to do with a specific combination will be numbered with the arabic number of the combination. Subsequent tables for the same combination will also be assigned a letter, in alphabetical order.

   Example: The first table for combination 1 will be Table 1. Subsequent tables will be Table 1A, 1B, etc. In general, Table 1 will give values in accepted engineering units and Table 1A will give the same values in SI units. For Combination 7, the first table will be Table 7, with SI units given in Table 7A.

2. Figures for each combination will be labeled first with the arabic number for the combination to which they refer and then with a letter in alphabetical order as follows:

XA = longitudinal tension

XB = transverse tension

XC = shear

XD = fatigue

X = 1 through 17

3. Other tables and figures which do not refer to any specific combination will be labeled with Roman Numerals in the order they occur.
4. All figures will give both systems of units on all axes.

Longitudinal Tensile Tests. Table II-1 summarizes the test results in Task II. Of the seventeen combinations tested there were six pairs of combinations which had the same composition in both the unidirectional and ± 15° panels: Combinations 1 and 9, 2 and 10, 3 and 11, 4 and 12, 5 and 13, and 7 and 14. Combinations 6 and 8 did not have corresponding ± 15° panels and combinations 15, 16 and 17 had 2024 Al as the matrix material instead of 1100 Al. Figures II-1A, B and C show the effect of temperature on longitudinal tensile strength as a function of fiber volume percent and fiber angle in the panel for the six pairs of comparable combinations.

Figure II-1A compares 8 mil B/W fiber panels at 50 and 60 v/o for both unidirectional and ± 15° panels. In this figure, the trends are masked by consolidation variations. C3 provided only room temperature (RT) specimens. The results for C11 at room temperature, the corresponding ± 15° panel, are suspect since the elevated temperature results are higher. In C1 and C9, the trend from RT to

149°C is similar: the scatter in the data makes it impossible to say there is an effect of temperature. For C1, at 260°C and 371°C it is also impossible to say that the drop in the average strength is solely due to temperature. The drop in strength at 260°C in C9 is more dramatic, 26% from RT, than for any other combination tested. It is likely that some of this decrease may be due to non uniform bonding.

Figure II-1B, similar to Figure II-1A, shows the results for 8 mil fiber when titanium foil is added on both surfaces and at the midplane of the composite. The room temperature strength of C4 is not as high as the strength of C3, the equivalent combination without titanium foils. The bonding of this panel was poor, yielding only three RT and one 149°C specimens. The addition of Ti, in every case, made achieving a sound bond more difficult. In C12 there seems to be a definite effect of temperature on tensile strength: a decrease of ∿15% between 149°C and 260°C. In C10 there is also evidence of a definite decrease in strength between RT and 371°C of ∿40%. These decreases, however, may also be reflecting the effect of poor bonds at the Ti and Al interface.

Figure II-1C shows the results for 5.6 mil fiber without titanium foils. This set of data is consistent and well behaved except for the fact that the 50 v/o, 0° combination is stronger than the 60 v/o combination. Although this figure shows that the average strength has decreased in all cases, the individual test results show that the scatter masks this apparent drop; this suggests that

it may be variations in the panel which are responsible for this result rather than an effect of temperature.

Figure II-2 compares the response of all the 0° combinations to elevated temperature. Note that the trend for C1, C5, C6 and C7 is very similar; the maximum apparent drop in average strength due to temperature occurred in C6 (∿14%). The average drop in strength for C1, C5 and C7 was 10% at 260°C. For C1 there was an additional apparent drop in strength at 371°C of ∿1%. Based on this data, the conclusion must be that there is a very slight decrease in 0° strength at 260°C, probably due to stress relief in the aluminum, and that there is only a slight decrease (∿1%) thereafter.

Figure II-3, similar to Figure II-2, shows the effect of temperature on the average strength of the ± 15° combinations. There is a definite effect of temperature on strength at temperatures above 149°C that cannot be explained by scatter in the data alone. This is to be expected because in the ± 15° combinations the matrix plays a larger role in composite strength and, above 149°C, the matrix starts to decrease in strength. The tensile modulus of all the combinations was approximately the value that a Rule-of-Mixtures (RoM) analysis would predict and, up to 149°C, did not decrease. Modulus and strain measurements were attempted on all samples at higher temperatures, but only edited results are shown in Appendix D. Since the strain gages start to be affected adversely by the high temperatures, giving erratic results, it was decided to report these values selectively.

Modulus Tests. Modulus values, in the longitudinal direction were generally at the level Rule of Mixtures would predict and did not seem to decrease appreciably at 149°C; in some cases the modulus actually appeared to increase. This may have been due to some type of stress relief caused by the higher temperature. Although specimens were strain gaged for modulus measurement at 260°C, the results were too erratic to report due to possible strain gage failures at the higher temperature.

Transverse Tensile Tests. Table II-2 shows that only two combinations containing Ti additions, out of a total of 7, yielded transverse specimens of sufficient quality to test. The Ti surface foils detached from the specimens during machining. In some cases debond occurred only at the midplane Ti-Al interface. Since this did not happen to longitudinal specimens it may be a stress-relief phenomenon.

Figures II-4 and II-5 show the effect of temperature on transverse tensile strength for both 5.6 mil and 8 mil fiber composites without Ti. The response of all combinations to elevated temperature in the 90° and ± 75° orientations is essentially the same and it does not seem to be dependent on fiber size. There is a large decrease in strength between RT and 149°C for the ± 75° orientation followed by another less severe, drop between 149°C and 260°C. The slopes are comparable regardless of volume percent reinforcement or fiber diameter.

In the 90° orientation the same may be true but the data are too limited to infer this conclusion. In general, the drop in strength of the 90° specimens between RT and 140°C is 13-20 percent; between 149°C and 260°C it is 12-29 percent. The drop in strength for the ± 75° specimens between RT and 149°C is 21-41 percent; between 149°C and 260°C it is 13-40 percent. Figures II-6 and II-7 show the similarity of the curves. Note that C8 and C10 contained Ti foil and had appreciably higher transverse strengths than similar specimens without Ti foil at all temperatures.

Figure II-8 compares the room temperature strength of all combinations versus composition of the combination. The combinations showed a definite strength dependence on fiber diameter (8 mil strongest) and fiber volume percent (60 v/o strongest) in both the 0° and ± 15° panel configuration. The same observations are not true for combinations made with 5.6 mil fiber. This may be because at high volume percent using 5.6 mil fiber the triaxial stress fields around the individual fibers begin to overlap due to smaller interfiber spacing thereby not allowing the fiber to contribute its full strength to the composite. A higher volume percent of 8 mil fiber, as compared to 5.6 mil fiber, can be obtained before this phenomenon occurs. In the ± 15° combinations there is very little difference in the strengths of all combinations in the longitudinal direction. In the transverse direction, the 8 mil fiber 0° combinations are weaker than the 5.6 mil 0° combinations. In the ± 15° combinations, without Ti additions, there is very little difference in transverse strength using either 5.6 or 8 mil fiber. The transverse strength of the ±15° combinations is higher than that of the 0° combinations.

At 260°C all combinations which contained no Ti additions decreased to approximately the same strength level: ∿30MPa (4.3 ksi) for 8 mil, 0° combinations, ∿43 MPa (6.2 ksi) for 8 mil ± 15° combinations and 54 MPa (7.8 ksi) for 5.6 mil ± 15° combinations.

Shear Tests. Table II-2 shows the results of all shear tests. The test specimens and rationale for using this type of test are described in Appendix B. The shear results for combinations 1-8 were calculated from the following equation (0° orientation):

$$\sigma_{s15°} \tilde{=} \frac{\sigma_B}{2} \text{ Sin } 2\Theta$$

where σ_s = shear stress at 15°

σ_B = Breaking load ÷ Total Area

Θ = 15°

so that $\sigma_{s15°} \tilde{=} \frac{\sigma_B \text{ Sin } 30°}{2}$

$$\tilde{=} \frac{\sigma_B}{4}$$

The specimens for combinations 9-17 (± 15° angleply orientation) were double-notch, the shear stress calculation for these was:

$$\sigma_{s_{\pm 15°}} \tilde{=} \frac{P}{A}$$

where P = Breaking Load

A = Thickness of specimen x distance between notches.

The results of the 15° off-axis specimens show that the shear strength is essentially the shear strength of the un-reinforced aluminum; this strength decreases with increase in temperature as the strength of aluminum decreases.

Although the test methods were different and the test results not directly comparable the results of the double notch shear tests on the ±15° panels suggest that the shear strength may have been at least doubled by the crossply. Note that most of the values show "greater than" signs. In most cases the distance between notches, 12.7 mm, was too large and the specimens failed in net section tension rather than in shear. Those specimens which did fail in shear are noted; in the case of C15 the notch distance was reduced to ∿7 mm so that the specimen would fail in a shear mode.

Fatigue Test Results. All fatigue tests were conducted with an MTS closed loop hydraulic test system Model 810. A 10,000 lb load cell was used. All tests were run in load control at a ration of minimum to maximum stress of R=0.1. For the room temperature tests a standard MRS extensometer was used to plot load versus strain for the first several cycles. For high temperature tests an extensometer could not be placed on the specimen so load-stroke was monitored.

The specimens was gripped by adhesively bonding soft aluminum tabs to the sample ends. These tabls were then placed in a clamp type grips. The high temperature tests required the specimen to be long enough that the tabs remained cool. There were very few sample failures at the grip indicating that the method was

successful. Samples were 609 mm (24 in) long for high temperature and 229 mm (9 in) long for room temperature tests.

For high temperature tests the sample was heated by a Keith Model 666 silicon carbide Globar furnace. The uniform temperature zone is 76 mm. Temperature was also checked periodically with Tempil-sticks marked on the specimen surface. All systems indicated the temperature was 260 $\pm$ 3°C.

The test plan was to attempt to choose stress levels that would give failures at 10^3, 10^4, 10^5, and 10^6 cycles. While this was not achieved on every material combination because of sample variability,the overall test results do span this range quite well.

As noted in Tables II-3 and II-4, the frequency of testing varied considerably. The first few cycles were run at 0.1 Hz to obtain the load-strain curves. The frequency was then stepped up slowly until maximum was reached. The maximum frequency at which a particular test could be run depended on the number of cycles to failure and on the total strain of the specimen. Fatigue data is plotted on Figures II-9 and II-10.

Fatigue Test. Combination 1: The four samples tested at room temperature were from two plates. The two plates exhibited such different fatigue life they do not appear to resemble each other at all. Similar results were obtained for the high temperature tests. Two specimens failed in the cold region and two in a warm region but not at 260°C. The scatter was tremendous for these four specimens. See Figure II-11 for photographs of fractures.

Combination 2: The four samples exhibited a consistent fatigue curve. Test temperature did not seem to be of much importance since some of the specimens failed in the hot zone and some outside the hot zone close to the grips without affecting the S/N curve (see Figure II-11).

Combination 5: The three samples that were tested in fatigue exhibited a consistent fatigue curve. Of the combinations tested this one had the best fatigue life with the exception of plate 31 of Combination 1. One sample failed prematurely on loading, the first cycle, at 1400 MPa. The reported tensile strength for this combination was 1503 $\pm$ 27 MPa. (See Figure II-12 for photograph of fractures.)

Combination 6: This combination exhibited a consistent fatigue curve. It appears to have considerably less fatigue life than Combination 5 which is similar except for the titanium enhancement. This can probably be explained by the fact that the titanium surface layer delaminated early in the test (see Figure II-12). Thus the actual stress being carried by the B/Al composite is higher than that given since the stress is calculated using the groos area of the composite without regard to the titanium delamination.

Combination 7: This combination exhibited a fairly consistent fatigue curve. Three of the samples would indicate that the increase from 50 v/o to 60 v/o decreases the allowable load at a given number of cycles about 10%. However, one of the samples

(RTLF 3) falls exactly on the curve for 50 v/o (Combination 5). The higher v/o makes the surface of the sample much worse looking during the progress of the test. Fibers are broken on the surface and the edges early in the test and continue to worsen during the test prior to failure (see Figure II-12).

Combination 8: Except for one sample this combination gave a consistent fatigue curve. The data also agrees very closely to combination 6 data indicating that for samples with titanium enhancement, the v/o of fiber does not seem to have much effect on fatigue life. Combinations 7 and 8 also exhibited very similar fatigue behavior indicating no effect due to titanium enhancement at the 60 v/o fiber content. (See Figure II-13 for photograph of fractures.)

Combination 10: This combination was the only one that seemed to be affected by the 260°C temperature. All four failures were in the hot region (see Figure II-11) and the shape of the sample changed during test. The tests also gave a consistent fatigue curve. The curve was almost identical with the room temperature Combination 12 tests. The only difference in the two combinations is 50 v/o versus 60 v/o and 260°C versus room temperature.

Combination 12: This combination exhibited a consistent fatigue curve. It was discussed in connection with Combination 10. Figure II-13 shows specimen fractures.

Combination 13: This combination gave very poor test results. All failures occurred in exactly the same relative place in the specimens indicating the tests were failing because of a poor spot in the plate. Also, all tests failed in the cold region.

Combination 14: This combination exhibited very mixed behavior. Two of the specimens closely matched the fatigue curve for the longitudinal tests. Two of the specimens closely matched the fatigue curves for $\pm$ 15° tests. (See Figure II-13 for fracture detail.)

General Summary Fatigue: For both the 0° and the $\pm$ 15° specimens, the combined results of each type test seemed to give the most consistent data if plotted as stress versus cycles. Attempts to correlate and plot the data as a percentage of tensile strength produced much more scatter. It is for this reason Figures II-9 and II-10 are plotted as they are.

A second general observation is that increasing the test temperature to 260°C (500°F) caused minimal change in fatigue life. This is shown by the data in Figures II-9 and II-10 and also by the fact that samples seemed to fail as readily in the cold zone as in the high temperature region.

A third general observation is that the modulus of elasticity changes from that obtained during the first application of load to a slightly higher value which is reached on the second and subsequent cycles. This change varied from specimen to

specimen but was about 5-20%. This behavior does not seem to affect stress levels, and did not seem to be greatly dependent on fiber volume percent. The exact modulus values cannot be given because the extensometers were not calibrated for this purpose; the stress-strain curves were plotted to follow the progress of the test and are not shown in this report.

For most metals it is possible to detect the initiation of a crack and follow its growth by following the change in the apparent strain during the fatigue test. This same procedure was followed on the composite materials. However, a crack initiation and growth was observed on only a few samples as noted in Tables II-3 and II-4. Most samples failed catastrophically without an apparent change in strain.

Thermal Expansion Test. Samples were supplied in the form of test coupons from fatigue or other tests. They were approximately 9.5 mm wide by the thickness of the various combinations. The thermal expansion samples were sheared from these pieces to about 7 mm long. The ends were smoothed on a belt sander.

The test apparatus was a Perkin Elmer Model DSC-1B differential scanning calorimeter with the TMA-1 thermal expansion unit. The instrument was calibrated with an aluminum standard sample to within $\pm$ 0.1 x 10^{-6} $°C^{-1}$. The unit is basically a quartz sample holder with a quartz rod resting on the sample. This rod is wider than the thickness of the samples. As the sample expands

the length change is measured by an LVDT and plotted directly onto the chart paper. Heating and cooling were controlled to 5.0 °C/min. The tests were designed to run from room temperature to 385°C (725°C). Test results are tabulated in Table II-5.

Results: All values shown in Table II-5 are calculated from the heating curve. There is a hysteresis effect in all samples. The hysteresis is small for C2 and C5, larger in C1, 8 and 9 and quite large in C10 and 13. The samples with fibers at $\pm$ 15° exhibited considerably larger hysteresis effects than did the samples with 0° fibers. These hysteresis effects have been reported previously for both B/Al and Gr/Al (Reference 18) and seem to be related to relief of residual stresses which are induced during cool-down from fabrication temperatures.

Results - Combinations 15, 16 and 17. Three combinations were made using 2024 Al. The results of static longitudinal and transverse tension and shear tests are given in Table II-2. Combination 15 gave good results at 149°C although bonding was erratic. This suggests that the low room temperature longitudinal strength was due to poor bonding. The transverse strength is comparable to C11 transverse strength at RT but decreases less rapidly at increased temperatures. The difference between C11 and C15 is only in the matrix used. The shear results for C15 are higher than for C11. Both combinations failed in shear. The longitudinal test results for C16 and C17 were very poor. The panels appeared very well bonded in the initial C-Scan. Fibers leached from these panels

and bend tested did not show a large enough decrease in strength to account for the poor strength. Nevertheless, some type of degradation must have taken place. Ordinary metallography and SEM work did not reveal the cause of these poor strengths. At the other extreme, the transverse strengths were quite good for these combinations. The transverse strengths were higher than any of the 1100 Al combinations which did not contain titanium and did not drop in strength at elevated temperature as fast as the 1100 Al composites.

GENERAL CONCLUSIONS

The results of this study warrant the following conclusions:

1. Although bonding parameters were not optimized for many of the seventeen combinations studied, it was demonstrated that B/Al can be produced by the air diffusion bonding process with mechanical properties which are equal to or better than properties obtained by the vacuum diffusion bonding process.
2. The mechanical properties of these composites are not significantly degraded by exposure to temperatures up to 371°C except for pure (90%) transverse strength which is highly matrix dependent.
3. In those combinations containing titanium, there was considerable difficulty in obtaining a sound bond. Where it was achieved the properties of the composite were very good. However, since titanium is an aggressive oxygen getter at high temperatures and the oxide layers on the Ti and Al hinder good bonding, using Ti enhancements in conjunction with air bonding is not recommended.
4. In the longitudinal direction, 8 mil fiber composites at 60 v/o produced high composite strengths and the properties of 8 mil fiber composites did show a dependence on fiber volume percent. However, 5.6 mil fiber composites did not show the same dependence. In transverse, shear and fatigue tests, the advantage of the 8 mil fiber at high volume percents was not seen. Overall, the 5.6 mil fiber produced better composite. The 1100 Al combination with the best all-around properties was 50 v/o, 5.6 mil B/W without Ti enhancement (C5 and C13).

REFERENCES

(1) Klein, M.J., et al., "Effect of Interfaces in Metal Matrix Composites on Mechanical Properties", Technical Report AFML-TR-72-226, Air Force Contract F33615-70-C-1814 (November 1972).

(2) Dolowy, J.F., Private Communication.

(3) Toth, I.J., et al., J. of Metals, 24 (12), 37-42 (1972).

(4) Dolowy, J.F. and Webb, B.A., "Al/B Composites Strengthening and Internal Mechanisms", SAMPE Quarterly, 2 (1), 62-67 (1970).

(5) Hersh, M.S. and Featherbey, M., "Joining of Boron/Aluminum Composites", J. Aircraft, 10 (2) 99 (1973). Also AIAA Paper No. 72-360 (1972).

(6) Metzger, G.E., "Joining of Metal-Matrix Fiber-Reinforced Composite Materials", Welding Research Council Bulletin 207 (1975).

(7) Burte, H.M. and Lynch, C.T., "The Technical Potential of Metal Matrix Composites", ASTM STP-438 (1968).

(8) Stuhrke, W.F., "The Mechanical Behavior of Aluminum/Boron Composite Material", ASTM STP-438 (1968).

(9) Burte, H.M. and Lynch, C.T., "Filament Matrix Compatibility", DMIC Memorandum 243, 1-6 (1969).

(10) Dolowy, J.F., "Fabrication and Processing Mechanisms Active in Aluminum/Boron Composites", DMIC Memorandum 243, 7-9 (1969).

(11) Stuhrke, W.F., "Solid State Compatibility of Boron/Aluminum Composite Material", DMIC Memorandum 243, 43-47 (1969).

(12) Davis, L.W. and Long, J.R., "Examining Composite Materials with the Scanning Electron Microscope", Metals Eng. Quarterly 12 (1), 38 (1972).

(13) McCall, J.L., "Fracture Analysis by Scanning Electron Microscopy", MCIC Report 72-12 (1972).

(14) Metals Handbook, 8th Edition, 9, Fractography and Atlas of Fractographs, ASM (1974).

(15) Kendall, E.G., Aerospace Corporation, and Davis, L.W., NETCO private communication.

(16) Phillips, B.F., "Secondary-Ion Mass Analysis: Instrumentation, Data, Interpretation, and Applications", J. Vac. Sci. Technol., 11 (6), 1093 (1974).

(17) Austin, A.E. and Phillips, B.F., "Investigations of Secondary Ion Mass Spectrometry", Battelle-Columbus Labs, Final Report to Naval Research Laboratory under Contract N00014-74-C-0266 (January 1975).

(18) Davis, L.W. and Sullivan, P.G., Final Report on "Exploratory Development of Graphite/Aluminum Composites", Contract N00024-75-C-5002, February 1976.

(19) Davis, L.W. and Sullivan, P.G., Final Report on "Exploratory Development of Graphite/Aluminum Composites", Contract N00024-76-C-5334, October 1977.

Table I-1. Compositions of Combinations Investigated.

Combination	Matrix Alloy	v/o	Fil Dia mils	Angleply Degrees	Titanium Matrix Enhancement
1	1100	50	8.0	0	No
2	1100	50	8.0	0	Yes
3	1100	60-65	8.0	0	No
4	1100	60-65	8.0	0	Yes
5	1100	50	5.6	0	No
6	1100	50	5.6	0	Yes
7	1100	60-65	5.6	0	No
8	1100	60-65	5.6	0	Yes
9	1100	50	8.0	± 15	No
10	1100	50	8.0	± 15	Yes
11	1100	60-65	8.0	± 15	No
12	1100	60-65	8.0	± 15	Yes
13	1100	50	5.6	± 15	No
14	1100	60-65	5.6	± 15	No
15	2024	60-65	8.0	± 15	No
16	2024	50	8.0	± 15	No
17	2024	50	5.6	± 15	No

Table I-2. Qualification Test Results - Tensile Tests.

Combination	Longitudinal MPa (ksi)	Transverse MPa (ksi)
1	1393 (202)	48.3 (7.0)
2	1358 (197)	146.9 (21.3)
3	1565 (227)	53.8 (7.8)
5	1027 (149)	175.1 (25.4)
8	1172 (170)	213.7 (31.0)
13	1048 (152)	82.0 (11.9)
14	1062 (154)	100.7 (14.6)

Table II-1. Details of Specimen Geometry.

Specimen Type	Specimen Geometry Width	Length	Comments
Room Temp Longitudinal and Transverse Tensile (all combinations)	9.5 mm (0.375 in)	152 mm (6 in)	Longitudinal-fibers parallel to length or 15° to length
Elevated Temp Longitudinal and Transverse Tensile (all combinations)	9.5 mm (0.375 in)	229 mm (9 in)	Transverse-fibers parallel to width or 15° to width
Room and Elevated Temperature Shear	13 mm (0.5 in)	229 mm (9 in)	Combinations 1-8 fibers at 15° to tensile axis Combinations 9-17 fibers parallel to tensile axis. Double notch specimen see Figure II-3C.
Room Temp Longitudinal Fatigue	9.5 mm (0.375 in)	229 mm (9 in)	Fibers parallel to length or 15° to length.
Elevated Temp Longitudinal Fatigue	9.5 mm (0.375 in)	610 mm (24 in)	

Table II-2. Summary of All Static Test Results - Task II.

Combination	LONGITUDINAL UTS/E* RT	300	500	700	TRANSVERSE UTS/E* RT	300	500	SHEAR* RT	300	500	700	NOTE
1	201.4/27.2	197.0/24.8	181.8/-	179.6/-	5.9/18.7	4.9/5.0	4.1/-	11.2	9.9	4.9		1
2	175.4/25.2	176.2/25.8	187.8/-	-		NOTE 2		12.4	11.1	10.9		
3	243.5/34.9	NOTE 2		-	8.1/20.7	7.0/20.9	5.0/-	13.4	-	12.4		
4	214.4/30.1	153.0/29.2										2
5	218.5/28.7	214.7/29.7	203.8/-	-	12.0/22.7	8.5/-.	-	11.1	5.9			
6	171.3/24.8	159.6/25.8	147.4/-	-		NOTE 2		14.2				
7	211.0/31.8	208.1/30	189.7/-	-		NOTE 2		5.5				
8	143.6/32.2	210.2/29.4	218.1/-	-	30.2/∿20	22.6/∿6	19.9/∿5	NOTE 2		10.3		
9	148.5/∿30	140.9/∿22	110.3/-	-	14.6/∿18	9.7/∿5	7.1/∿3	19.3 (shear failure)	12.3	-	12.3	3
10	66.6/- Debond	126.1/∿25	-	-		NOTE 2		>20.4	>21.1	-		4
10A	140.8/24	109.9/-	109.6/-	92.6/-	24.6/16.1	19.3/∿11	16.7/∿6	-	-	>16.9		4&5
11	96.8/36.5	155.9/25.4	∿143/-	-	13.9/-	8.2/8.2	6.3/-	24.4 (shear failure)	24.6	-		
12	154.8/27.4	164.4/28.4	139.1/-	-		NOTE 2		>21.8	>24.			4
13	149.4/25.9	134.8/25.1	126.3/-	-	20.5/-	13.2/-	7.9/-	>17.2	>17.	>16.6		4
14	161.2/28.4	160.7/∿26	160.0	-	15.1/-	9.8/-	6.9/-		>14.			4
15	148.0/32	180.0/∿33	121.2/-	-	13.7/∿30	11.6/∿19	10.9/-	25.4 (shear failure)	32.2	29.5		
16	39.3/27.8	34.8/22.9	30.0/-	-	21.1/20.0	21.7/22.3	17.5/-	>11.0	>8.4	>6.3		4
17	58.7/25.0	58.0/26.0	51.0/-	-	18.0/∿20	18.6/∿20	15.4/∿20	>10.3	>9.7			4

NOTE 1: 500°F shear specimen did not fail in shear - specimen necked and failed net section tension.

NOTE 2: Panel debonded - most specimens not suitable for test.

NOTE 3: Shear tests for combinations 1 through 8 were 15° off-axis specimens; shear tests for combinations 9 through 15 were double notch specimens

NOTE 4: Shear specimens did not fail in shear - notches too far apart (0.5").

NOTE 5: This combination remade.

*: UTS in ksi

E in Mpsi

Table II-3. Summary of Room Temperature Fatigue Results on Various B/Al Composite Combinations. All Tests Run at R = 0.1.

Specimen	Dimensions Inches	Max Stress ksi	Max Frequency Hz	Cycles to Failure	Comments
Combination 1: 50 v/o - 8.0 mil filament					
RTLF 1 (plate 30)	.077 x .375	175	11	11,170	Surface broken at 3200 cycles; broke at center and in grips, delaminated
RTLF 3 (plate 30)	.077 x .379	150	11	3,080	Crack initiation at 2300 cycles, delaminated
RTLF 1 (plate 31)	.064 x .378	150	11	373,230	Looked good throught test
RTLF 2 (plate 31)	.064 x .374	190	32	788,290	Surface cracking at 52,000 cycle
Combination 5: 50 v/o - 5/6 mil filament					
RTLF 1	.058 x .375	190	11	3,410	
RTLF 2	.057 x .376	164	6	25,770	Crack initiation at 10,000 cycle, surface partially broken at 24,000 cycles
RTLF 3	.058 x .377	140	37	356,350	Cracking at edges at 222,000 cycles, failed at grip
RTLF 4	.057 x .374	-	-	-	Failed at 203 ksi on 1st cycle
Combination 6: 50 v/o - 5.6 mil filament - Ti enhancement					
RTLF 1	.063 x .378	137	11	67,080	Permanent offset in each cycle for first 20 cycles; surface delamination
RTLF 2	.063 x .371	154	32	23,440	Delaminated at 16,700 cycles
RTLF 3	.062 x .375	103	32	324,860	Surface delaminated; broke close to grip
RTLF 4	.061 x .376	94	37	>2 x 10^6	Did not fail

Table II-3 Continued

Specimen	Dimensions Inches	Max Stress ksi	Max Frequency Hz	Cycles to Failure	Comments
Combination 7: 60 v/o - 5.6 mil filament					
RTLF 1	.050 x .377	180	1	1,400	Edges broken at 100 cycles
RTLF 2	.050 x .375	135	11	65,750	Surface fibers broken at 180 cycles, surface broken up at 33,000 cycles, crack initiation at 65,300 cycles
RTLF 3	.050 x .375	157	11	69,490	Fibers loose on edges at 90 cycles; surface broken up at 30,000 cycles; crack initiation at 68,000 cycles
RTLF 4	.050 x .375	120	30	$>5.245 \times 10^6$	Fibers broken on edges at 16,000 cycles; surface broken up at 10^6 cycles
Combination 8: 60 v/o - 5.6 mil filament - Ti enhancement					
RTLF 1	.062 x .377	160	0.1	4	Surface layer was loose before test, failed in grip
RTLF 2	.061 x .376	160	11	11,980	
RTLF 3	.061 x .376	140	11	53,530	Surface layer delaminated
RTLF 4	.061 x .371	180	0.1	270	Permanent offset in each cycle for first 10 cycles; surface layer delaminated

Table II-3 Continued

Specimen	Dimensions Inches	Max Stress ksi	Max Frequency Hz	Cycles to Failure	Comments
Combination 12: ± 15° - 60 v/o - 8.0 mil filament - Ti enhancement					
RTLF 1	.081 x .376	124	0.1	145	Crack initiation at 45 cycles, audible cracking in last 10 cycles
RTLF 2	.082 x .378	93	37	2,360	Permanent offset in each cycle for first 20 cycles
RTLF 3	.083 x .378	77.5	37	5,200	
RTLF 4	.082 x .379	46.5	46	290,210	Broke in grip
Combination 14: ± 15° - 60 v/o - 5.6 mil filament					
RTLF 1	.051 x .374	128	37	53,660	
RTLF 2	.051 x .375	145	37	16,720	Permanent offset in each cycle for first 30 cycles
RTLF 3	.050 x .375	115	0.1	160	Audible cracking in first cycle with permanent offset each cycle
RTLF 4	.052 x .375	97	0.1	300	Audible cracking in first cycle

Table II-4. Summary of 260°C (500°F) Fatigue Results on Various B/Al Composite Combinations. All Tests Run at R = 0.1.

Specimen	Dimensions Inches	Max Stress ksi	Max Frequency Hz	Cycles to Failure	Comments
Combination 1: 50 v/o - 8.0 mil filament					
HTLF 1	.074 x .376				Failed in cold region on first cycle at 136.6 ksi
HTLF 2	.074 x .376	144	10	5,050	Failed adjacent to grip in cold region
HTLF 3	.074 x .376	120	25	535,560	Specimen was delaminated in middle near end before test failed slightly outside the 500°F region
HTLF 4	.073 x .376	145	10	820	Same as HTLF 3
Combination 2: 50 v/o - 8.0 mil filament - Ti enhancement					
HTLF 1	.097 x .375	150	10	33,440	Surface layer broken at 24,000 cycles
HTLF 2	.097 x .377	170	10	1,640	Failed in a common region but below 500°F
HTLF 3	.097 x .377	130	13	120,040	Surface layer broken at 35,000 cycles, failed in common region but below 500°F
HTLF 4	.097 x .375	120	12	166,170	Failed in 500°F region
Combination 10: 50 v/o - 8.0 mil filament - Ti enhancement - ± 15°					
HTLF 1	.096 x .377	80	15	4,790	Center section in bottom zone warped after test failed in 500°F region
HTLF 2	.097 x .376	88	12	3,500	Same as HTLF 1
HTLF 3	.096 x .376	60	28	26,980	Same as HTLF 1
HTLF 4	.098 x .374	40	30	43,820	Same as HTLF 1

Table II-4 Continued

Specimen	Dimensions Inches	Max Stress ksi	Max Frequency Hz	Cycles to Failure	Comments
Combination 13: 50 v/o - 5.6 mil filament - ± 15°					
HTLF 1	.059 x .377				Failed in cold region on first cycle at 51.3 ksi
HTLF 6	.056 x .374				Failed in cold region on first cycle at 69.2 ksi
HTLF 7	.057 x .376	60	0.1	30	Failed in cold region
HTLF 8	.057 x .378	30	30	84,810	Failed in cold region (all of combination 13 specimens failed at exactly the same place - 4 1/2 inches from right end of specimen.)

Table II-5. Summary of Thermal Expansion Results on Various B/Al Composite Combinations

Combination	Thickness Inches	Length Inches	α $°C^{-1}$	Comments
1	0.077	0.293	20-200 = 5.9×10^{-6}	Some hysterisis effect on cooling
			200-400 = 7.6×10^{-6}	
2	0.097	0.341	20-400 = 6.2×10^{-6}	
5	0.058	0.268	20-200 = 19.6×10^{-6}	Measured in transverse direction
			200-400 = 22.5×10^{-6}	
8	0.062	0.281	20-400 = 5.7×10^{-6}	Some hysterisis effect on cooling
9		0.273	20-400 = 4.9×10^{-6}	" "
10	0.096	0.282	20-400 = 4.6×10^{-6}	" "
13	0.057	0.247	20-200 = 5.4×10^{-6}	begins to decrease above 220°C, and reaches zero at 345"C. The specimen then contracts to 400°C

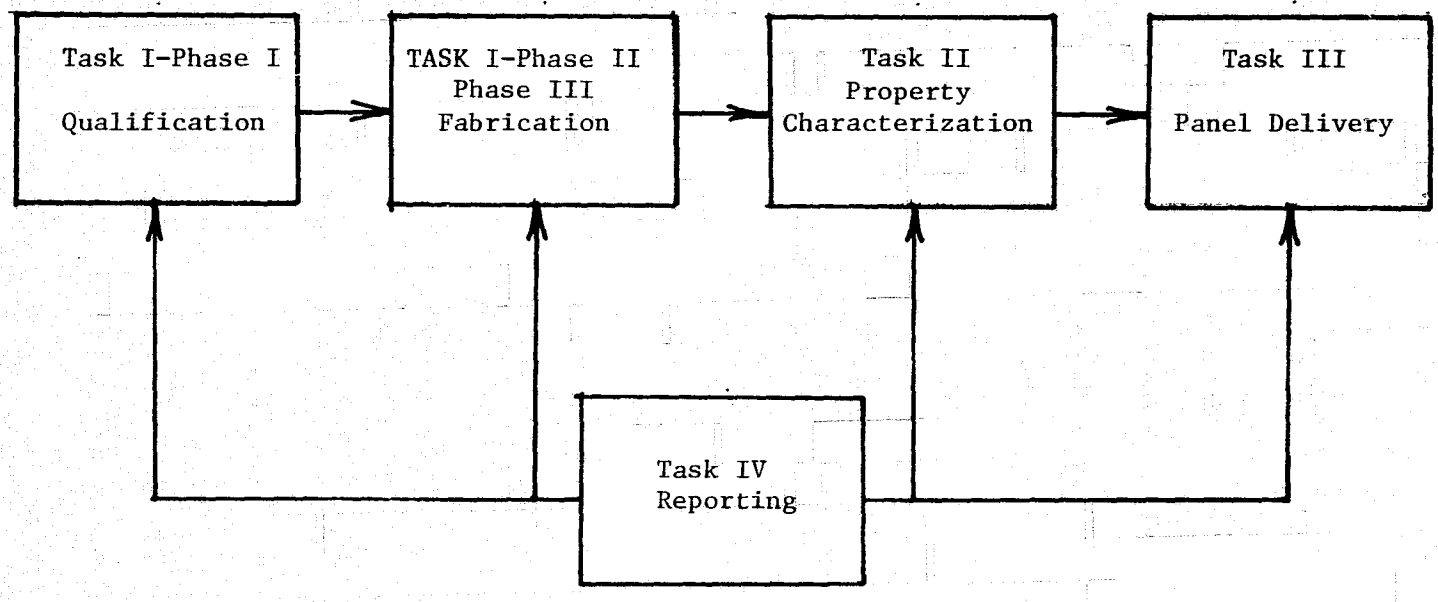

Program Organization
FIGURE I

FIGURE II-1A
EFFECT OF TEMPERATURE ON LONGITUDINAL STRENGTH AS A FUNCTION OF FIBER V/o AND ANGLEPLY

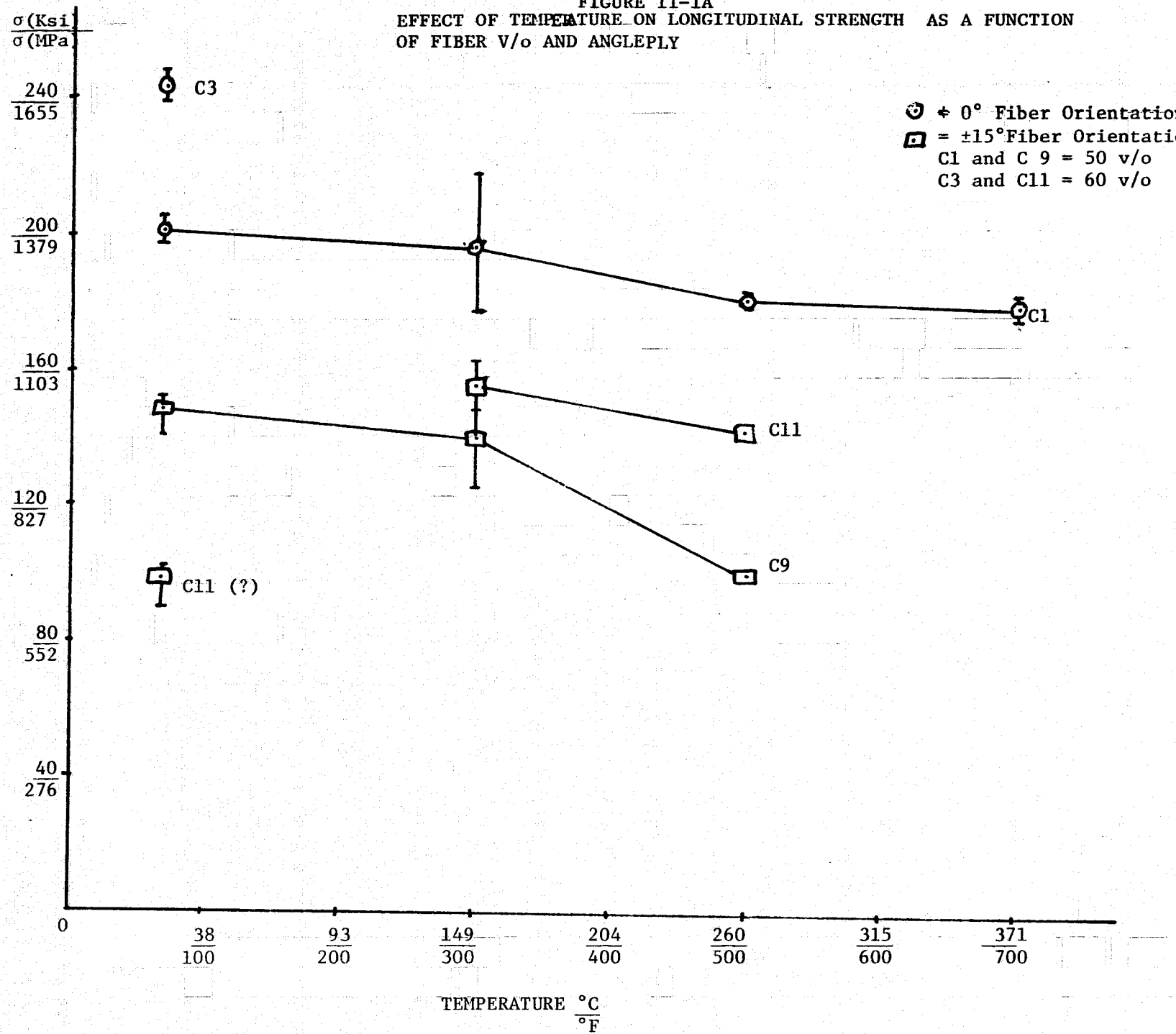

FIGURE II-1B
EFFECT OF TEMPERATURE ON LONGITUDINAL STRENGTH AS A FUNCTION OF FIBER V/o and ANGLEPLY

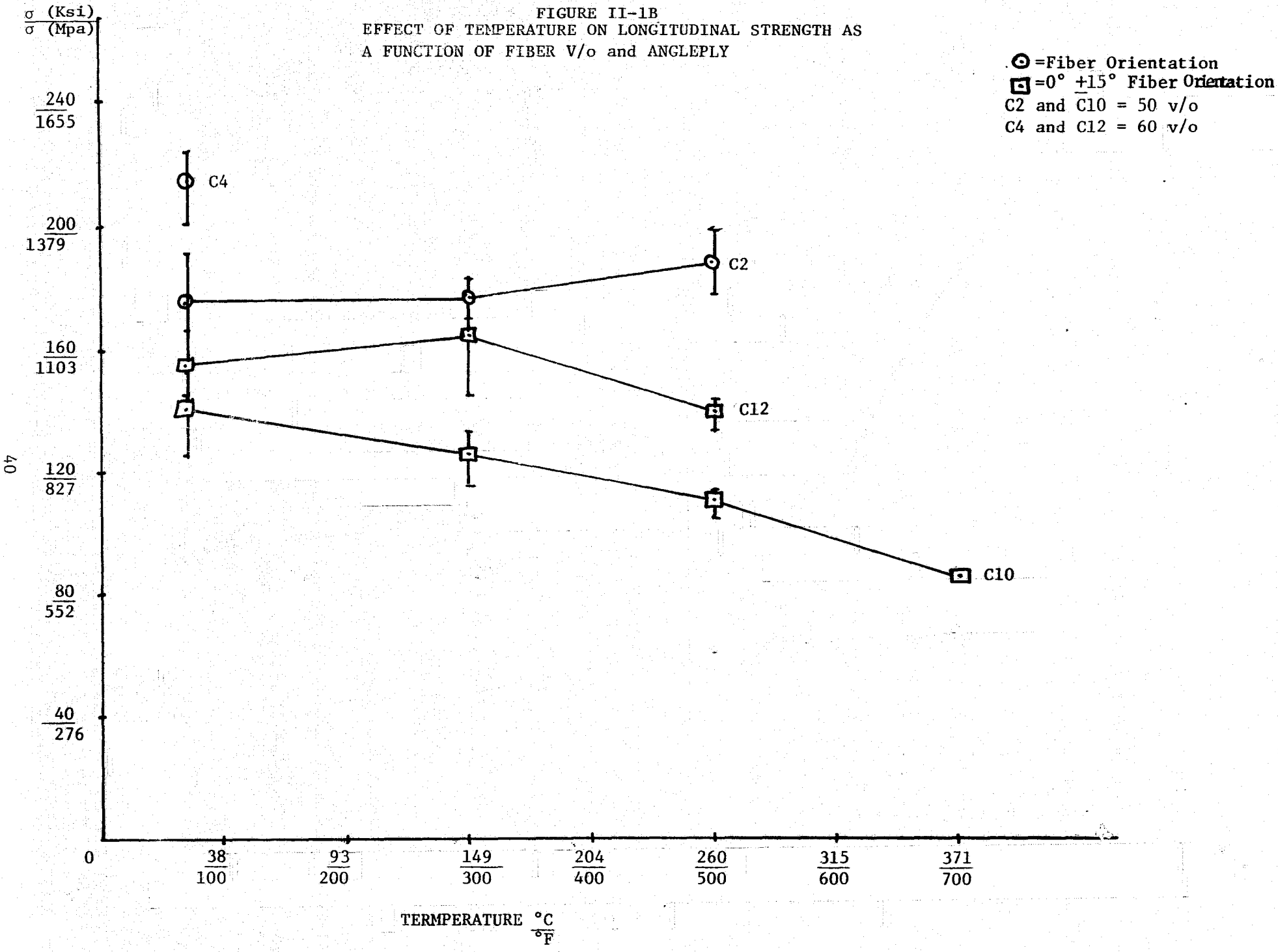

FIGURE II 1-C . EFFECT OF TEMPERATURE ON LONGITUDINAL STRENGTH AS A FUNCTION OF FIBER V/O AND ANGLE

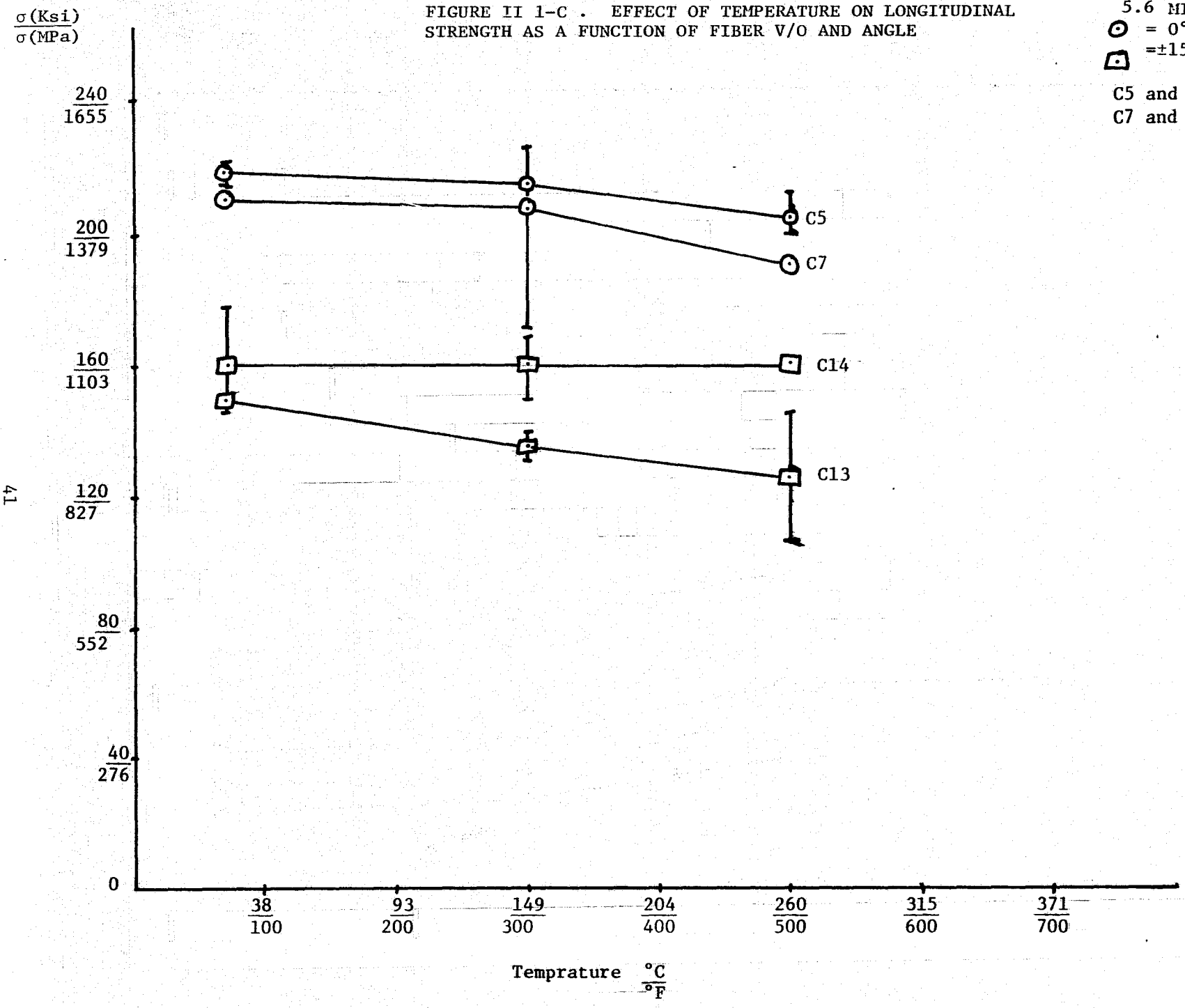

FIGURE II-2

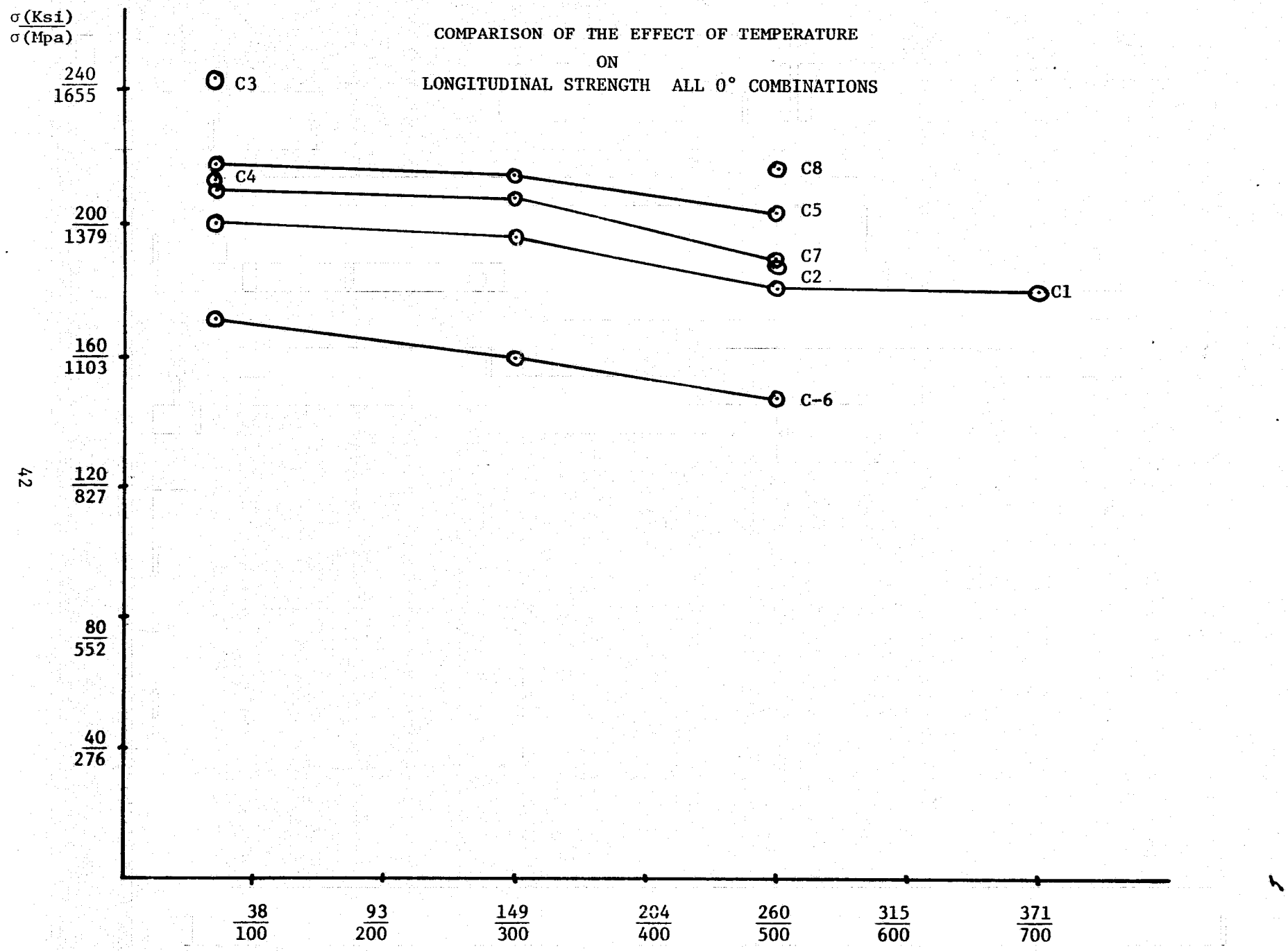
σ (Ksi)
σ (Mpa)
COMPARISON OF THE EFFECT OF TEMPERATURE
ON
LONGITUDINAL STRENGTH ALL 0° COMBINATIONS
240
1655
200
1379
160
1103
120
827
80
552
40
276
C3
C4
C8
C5
C7
C2
C1
C-6
38
100
93
200
149
300
204
400
260
500
315
600
371
700

COMPARISON OF THE EFFECT OF TEMPERATURE
ON
LONGITUDINAL STRENGTH OF ±15° COMBINATIONS

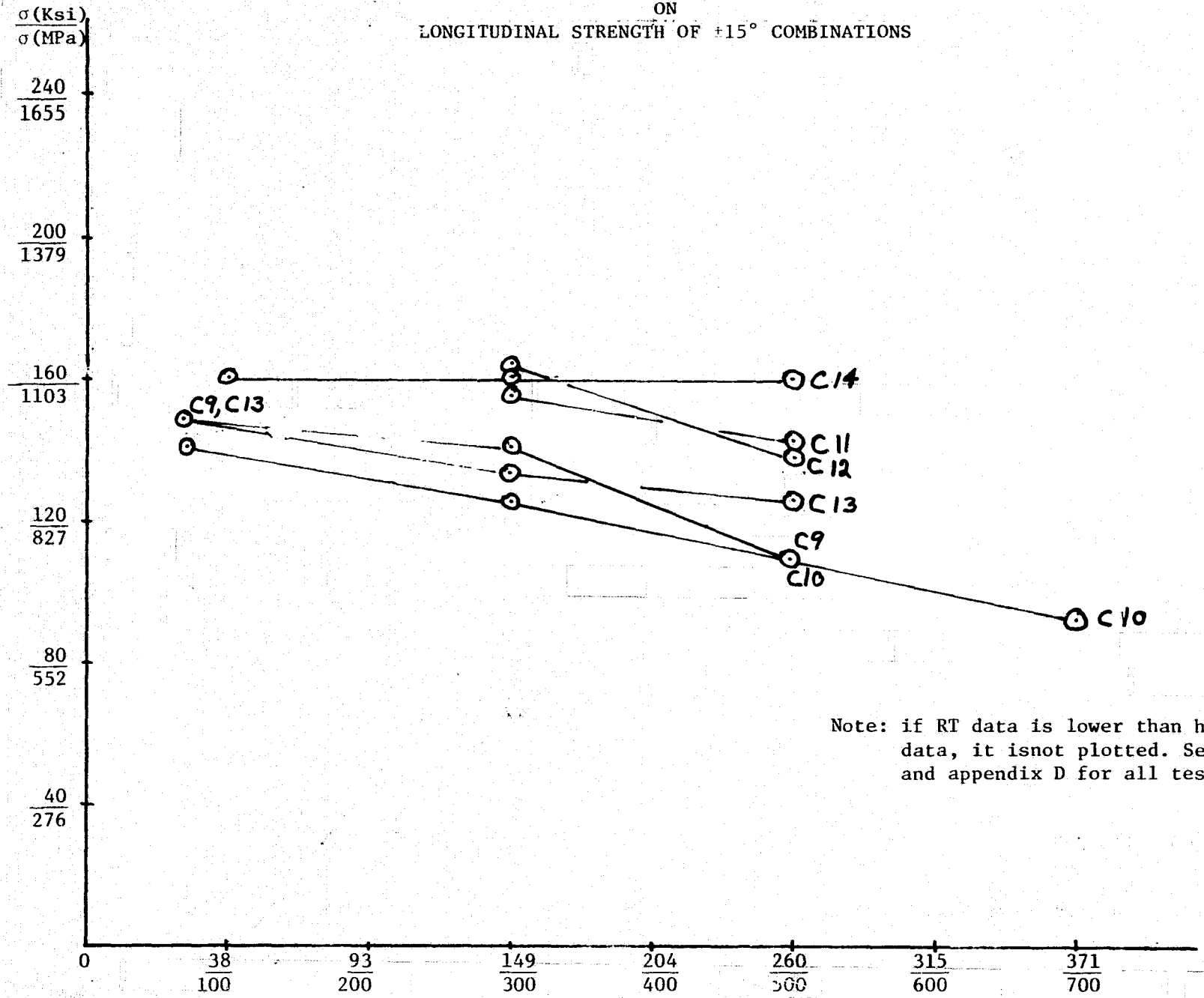

Note: if RT data is lower than high temp data, it isnot plotted. See Table II and appendix D for all test results.

FIGURE II-4
EFFECT OF TEMPERATURE ON TRANSVERSE STRENGTH
AS A FUNCTION OF FIBER v/o AND ANGLEPLY

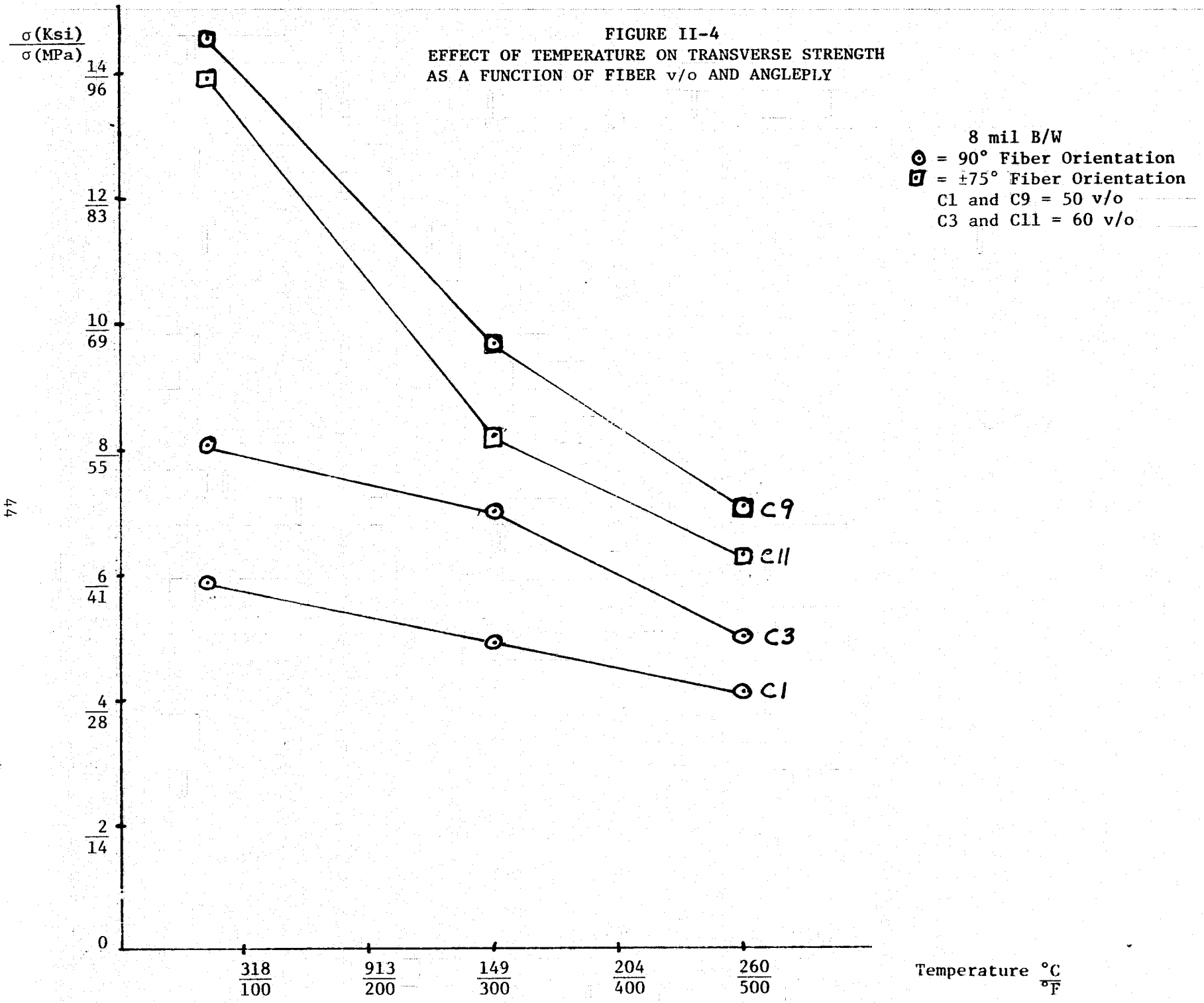

FIGURE II- 5

EFFECT OF TEMPERATURE ON TRANSVERSE STRENGTH AS A FUNCTION OF FIBER v/o AND ANGLEPLY

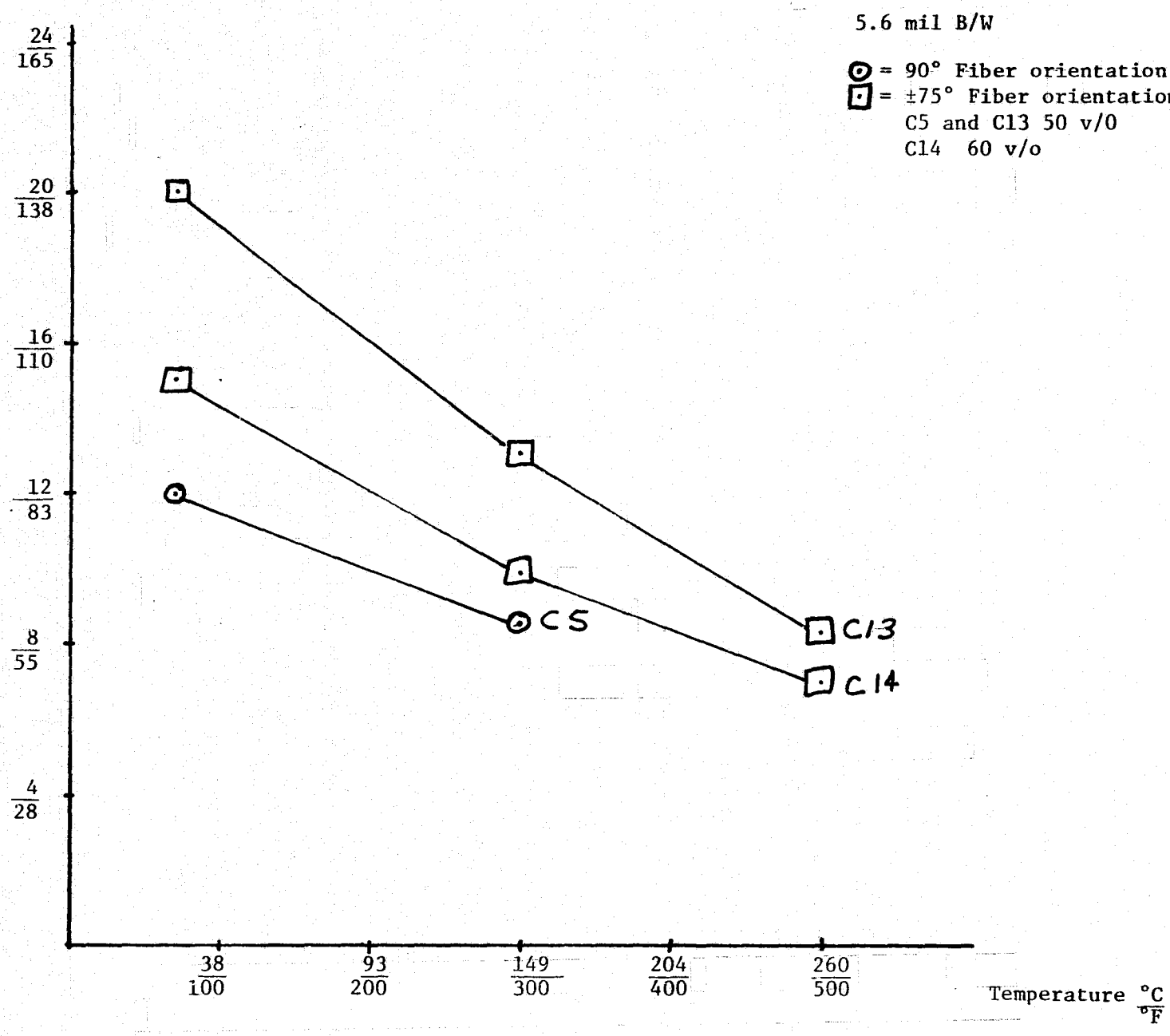

FIGURE II-6

COMPARISON OF THE EFFECT OF TEMPERATURE ON TRANSVERSE TENSILE STRENGTH UNIDIRECTIONAL PANELS

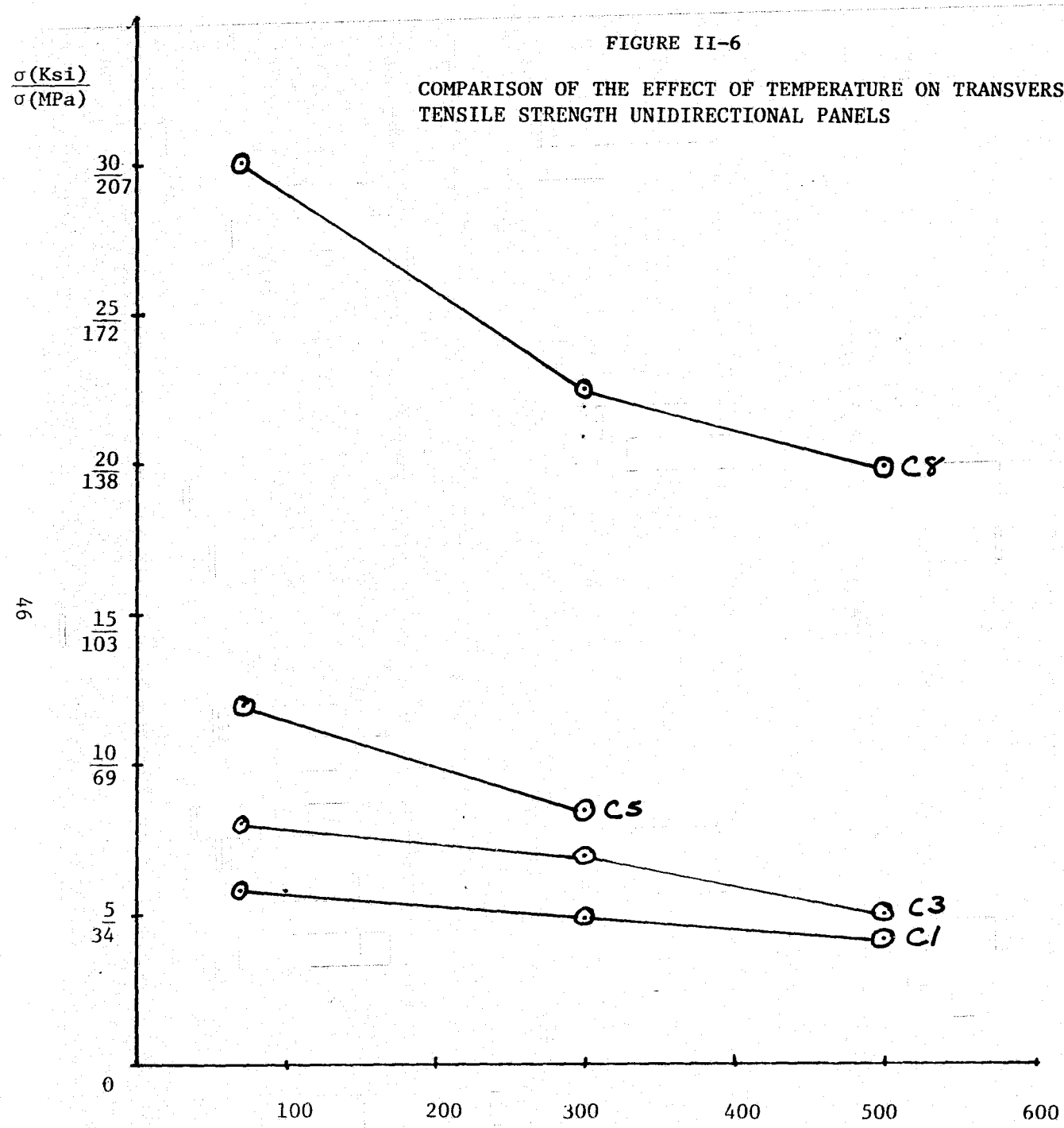

FIGURE II-7

COMPARISON OF THE EFFECT OF TEMPERATURE ON TRANSVERSE TENSILE STRENGTH ±15° PANELS

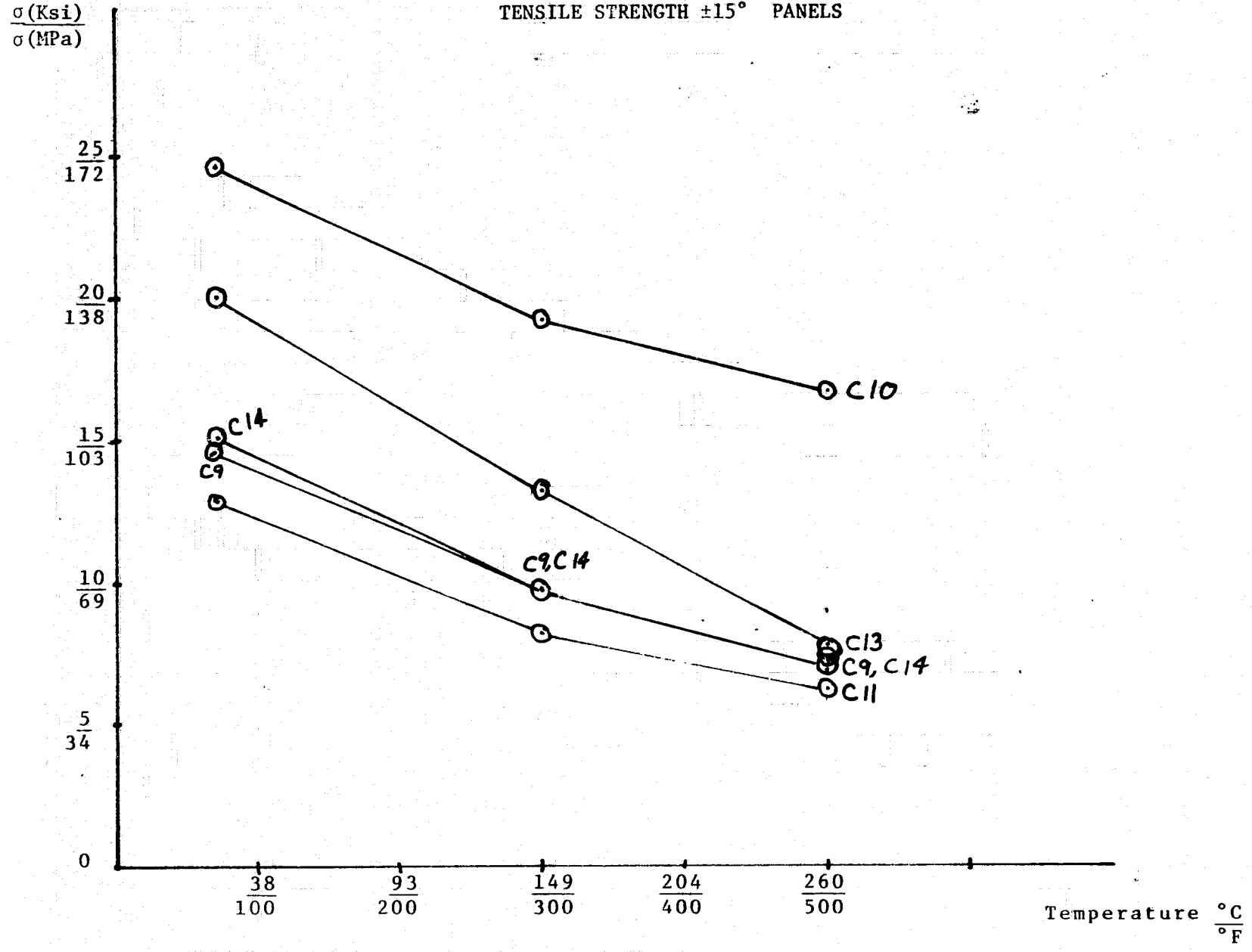

FIGURE II-8
COMPARISON OF RT STRENGTH OF ALL COMBINATIONS
IN LONGITUDINAL AND TRANSVERSE DIRECTIONS

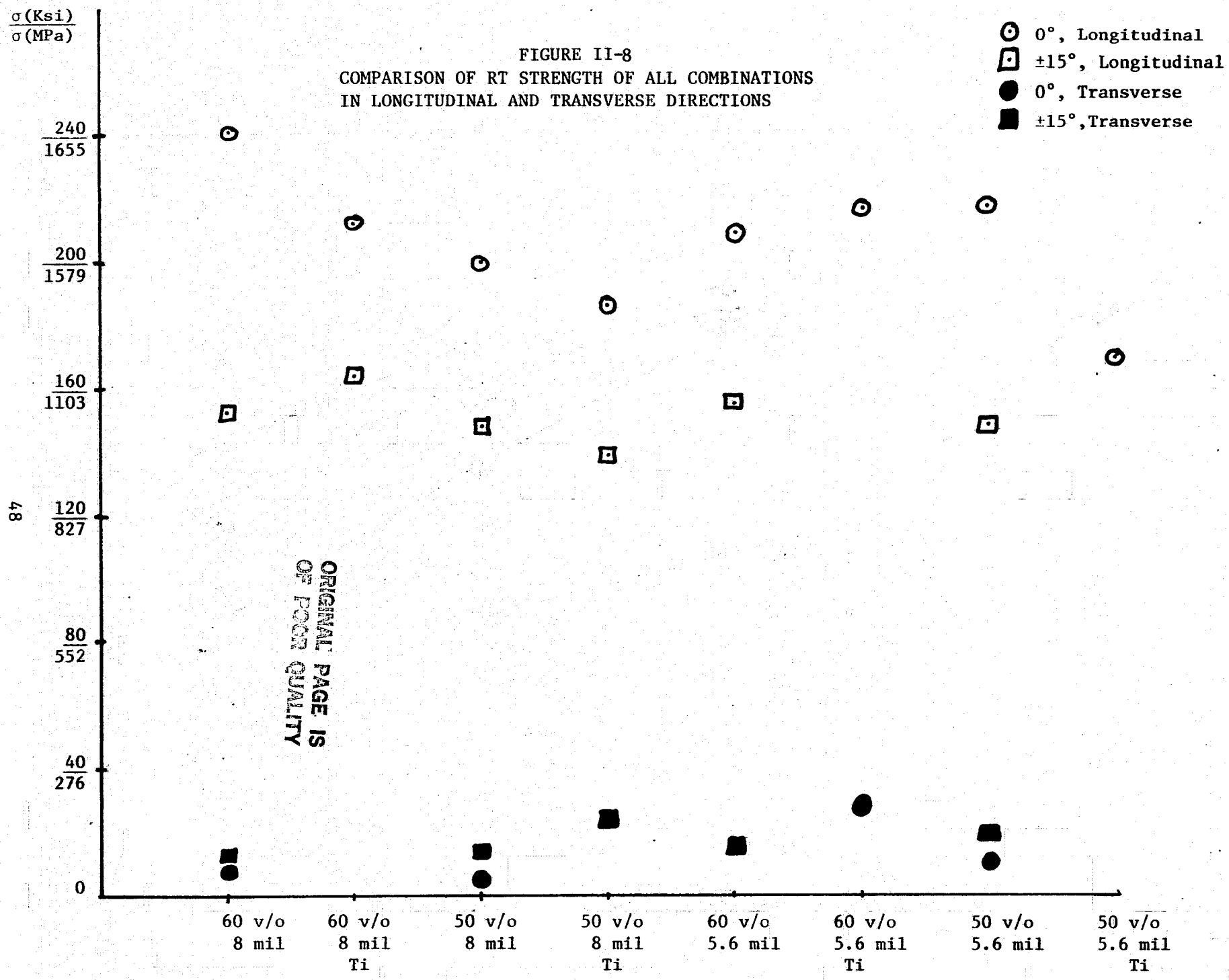

Figure II-9. Fatigue Test Results for Unidirection Combinations.

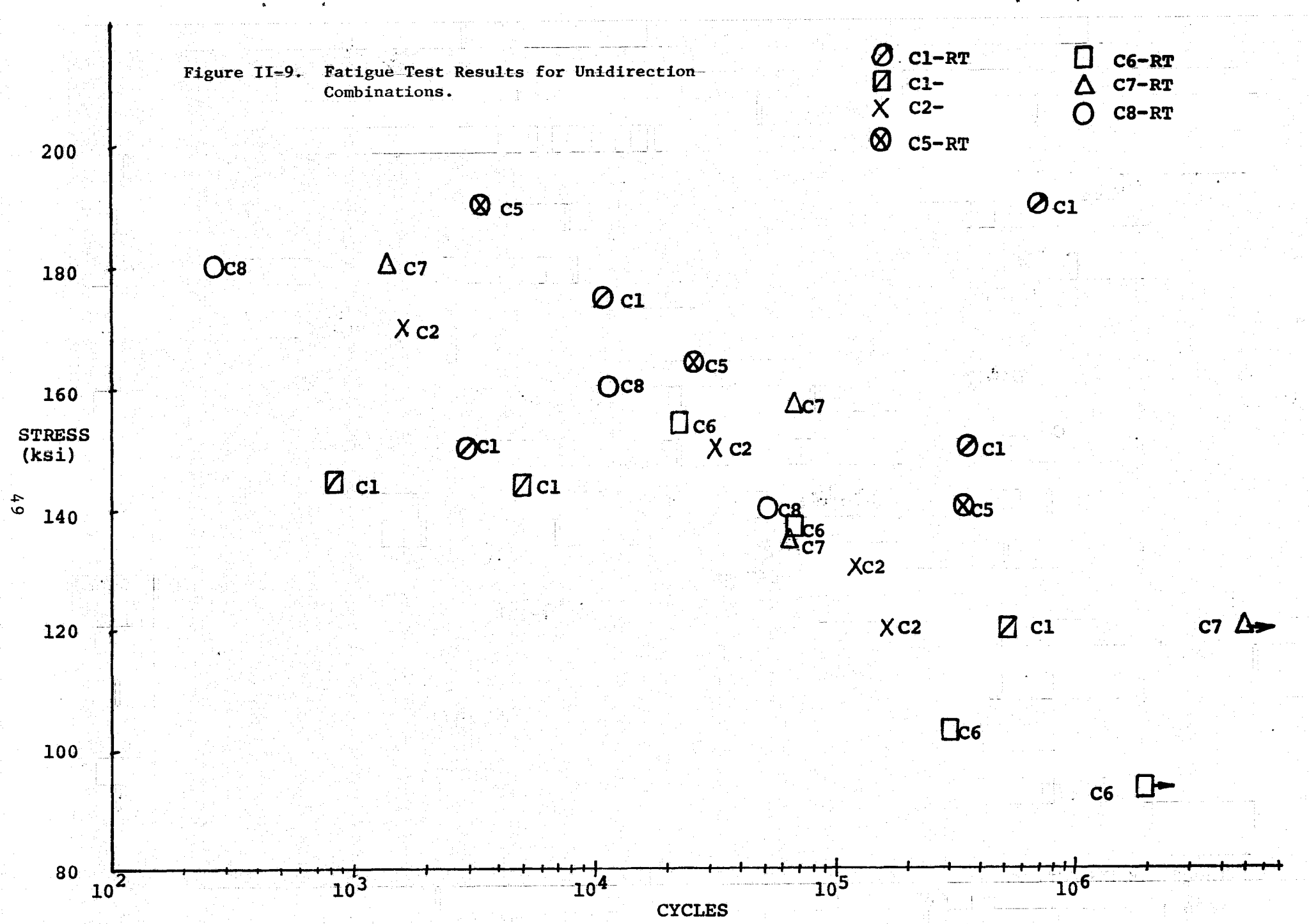

Figure II-10. Fatigue Test Results for ± 15° Combinations.

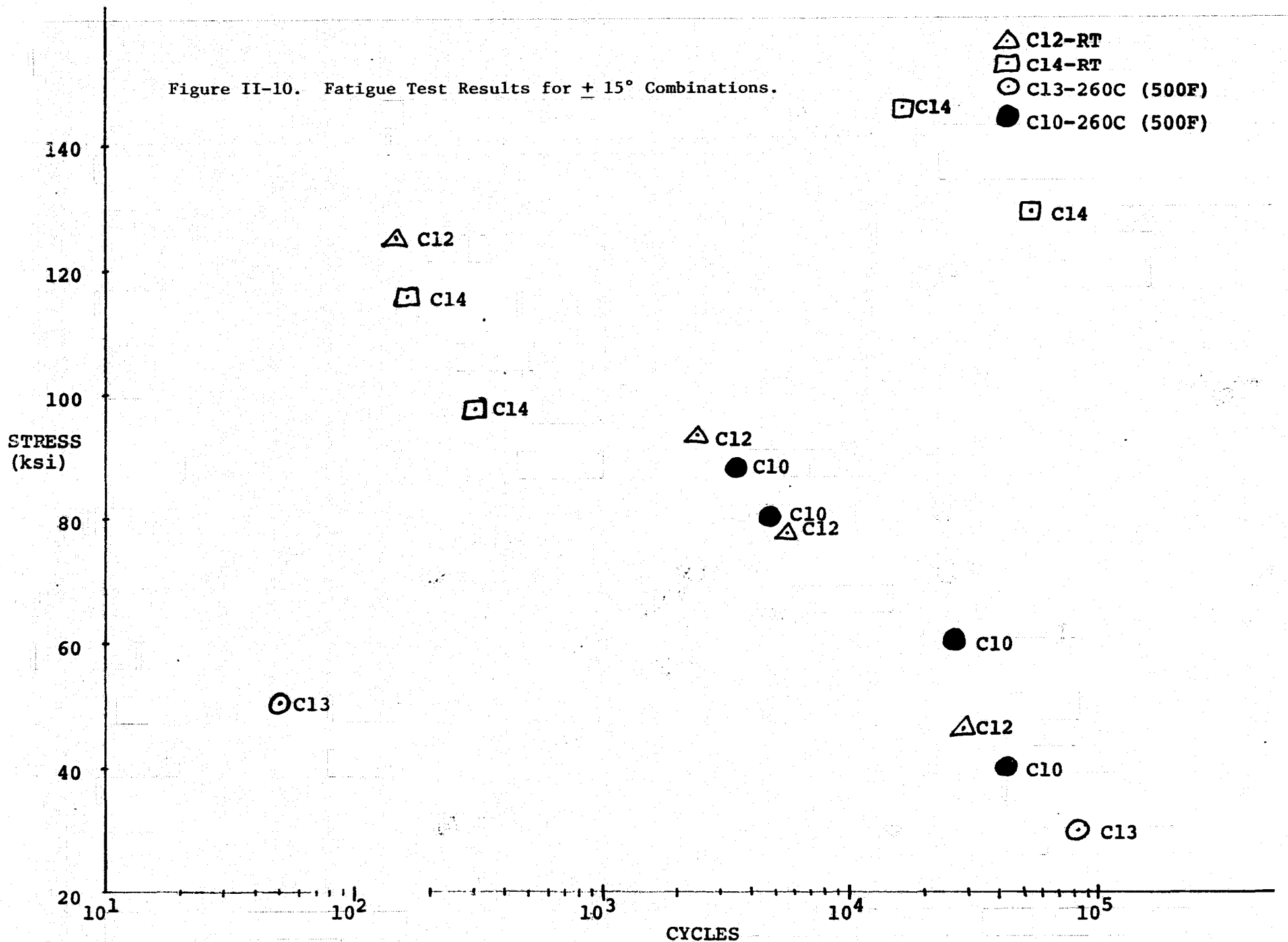

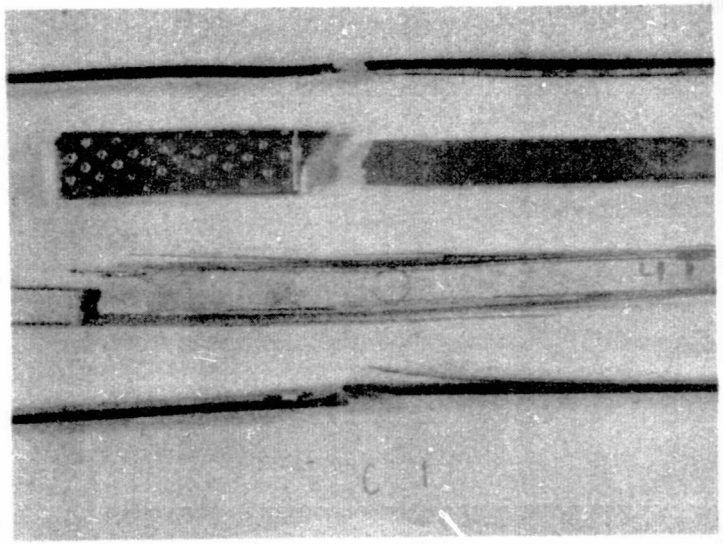

(a)

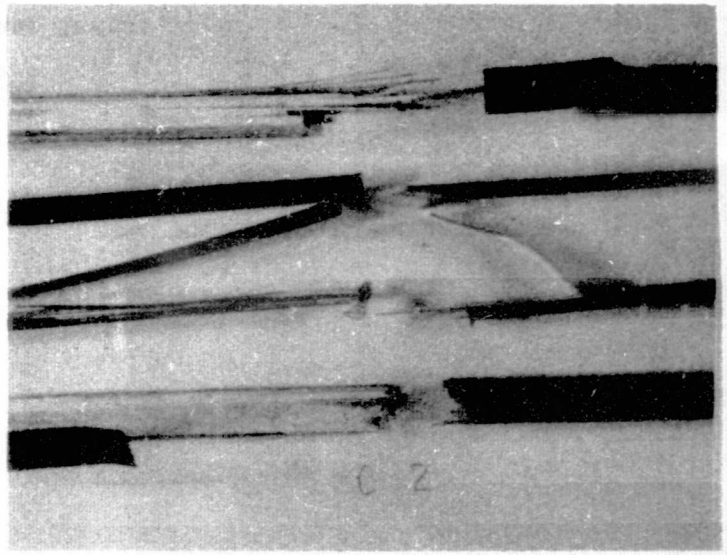

(b)

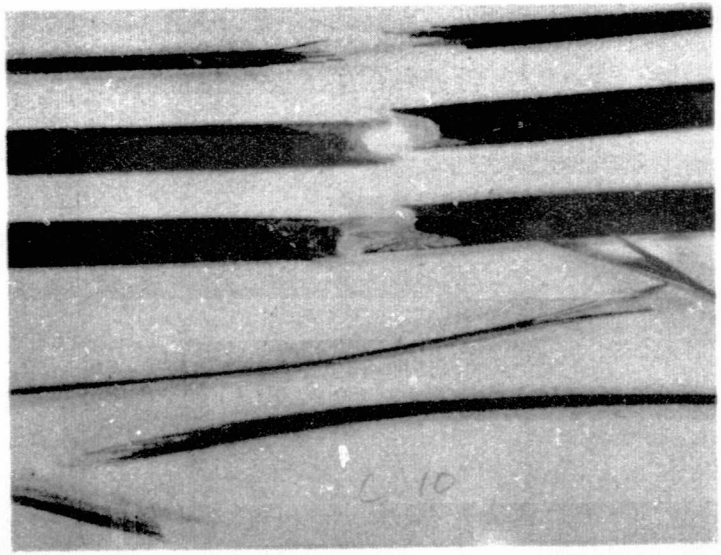

(c)

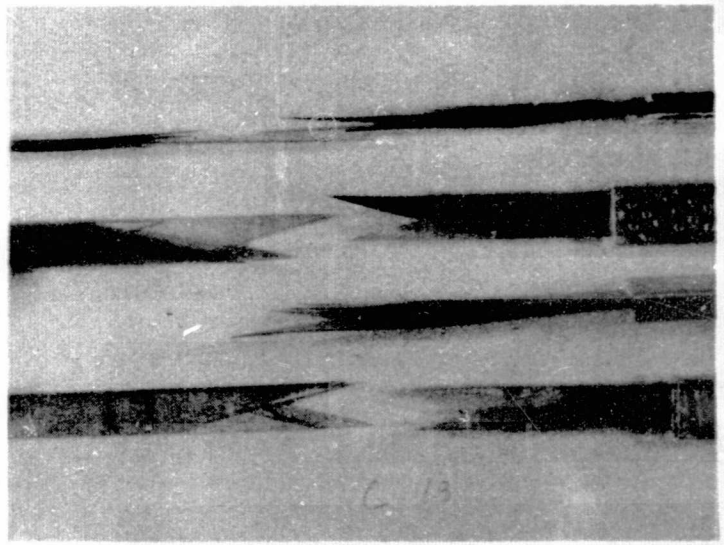

(d)

Figure II-11. Photographs of Failed 260°C (500°F) Fatigue Tests:

(a) Combination 1, (b) Combination 2, (c) Combination 10, and (d) Combination 13.

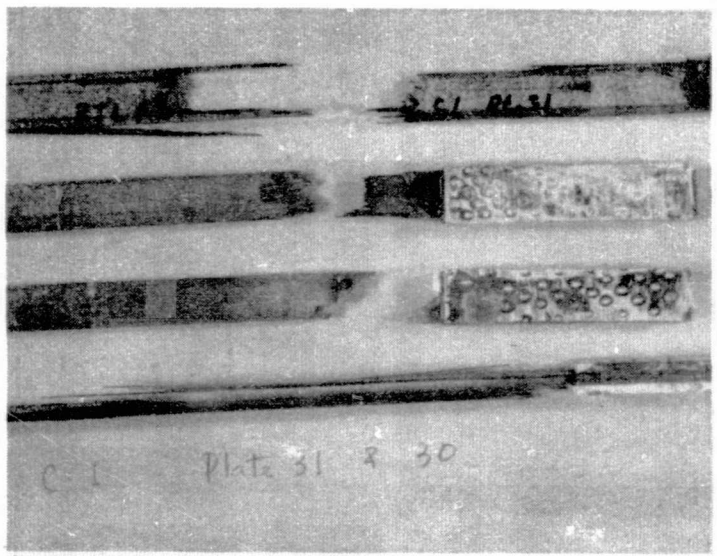

(a)

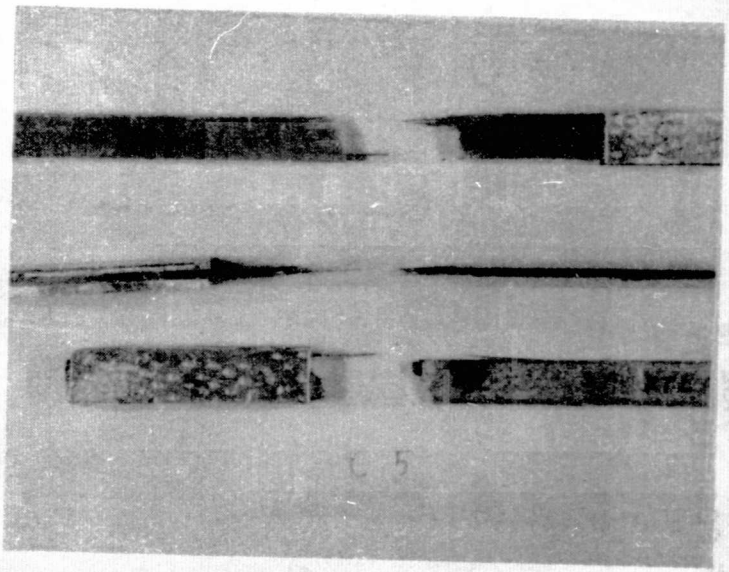

(b)

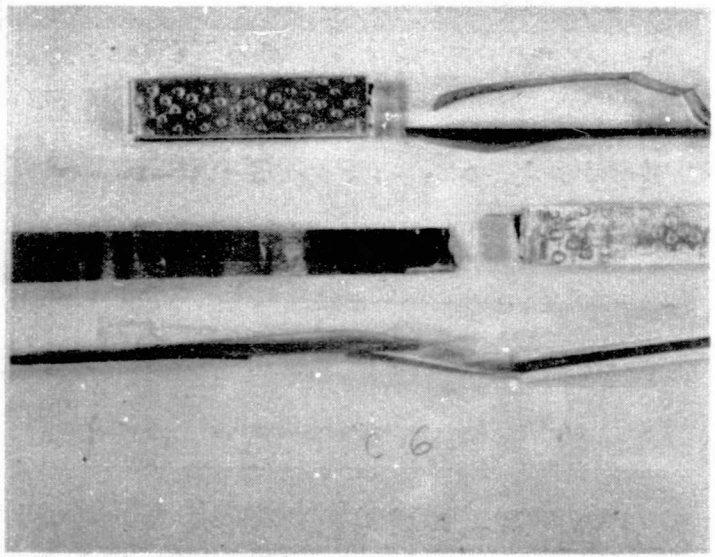

(c)

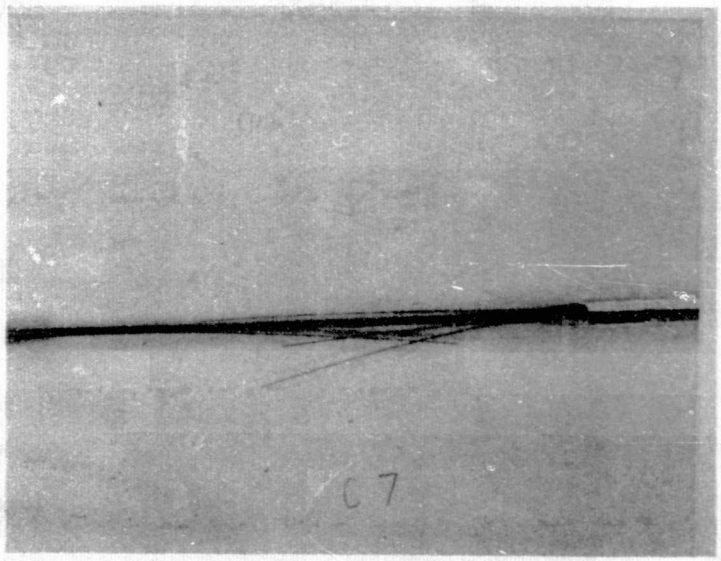

(d)

Figure II-12. Photographs of Failed Room Temperature Fatigue Tests:

(a) Combination 1, (b) Combination 5, (c) Combination 6, and (d) Combination 7.

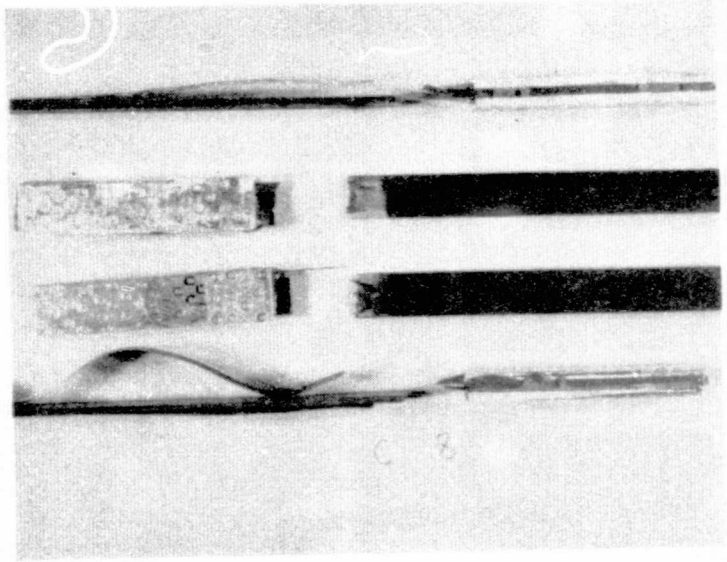

(e)

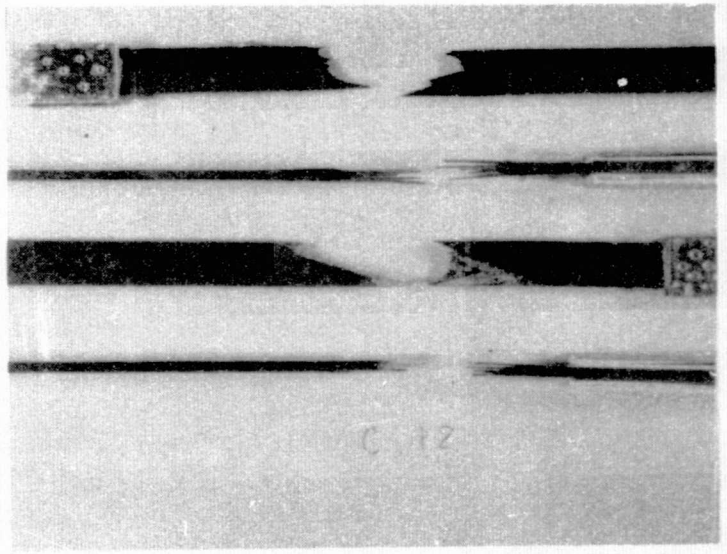

(f)

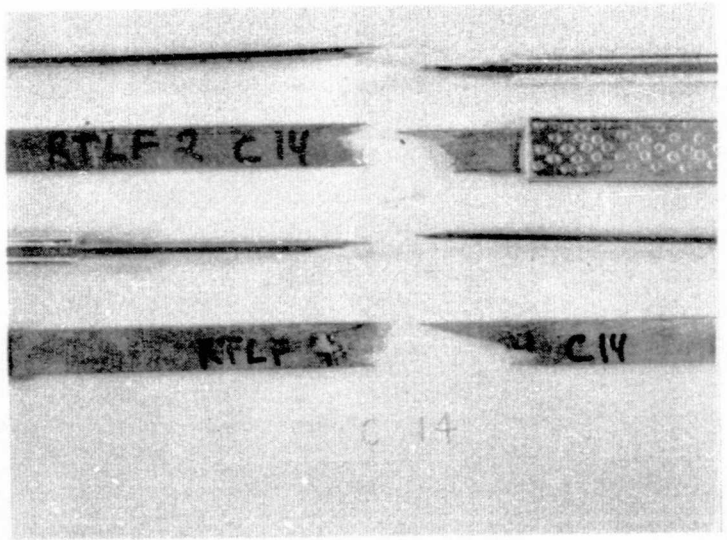

(g)

Figure II-13. Photographs of Failed Room Temperature Fatigue Tests (continuation of II-12): (e) Combination 8, (f) Combination 12, and (g) Combination 14.

APPENDIX A

APPENDIX A

DESCRIPTION OF NON-DESTRUCTIVE TEST (NDT) METHODS

All of the incoming B/Al material was visually inspected for surface defects and then inspected by ultrasonic C-Scan and standard radiography techniques. If only one NDT method was used, it was the C-Scan.

It was found, after several panels had been inspected, that the C-Scan technique yielded the most pertinent information and that radiography merely confirmed the C-Scan results. For this reason, the rest of the panels were inspected by C-Scan only.

Procedure

In the C-Scan technique the specimen is fully immersed in a water bath. In this case, the panels were placed on blocks on top of a 6 mm thick glass plate. The equipment consisted of a Uresco bridge and a Bronson 600 scope. A lithium sulfate, 10 MHz, 19 mm (3/4 in) medium focus (25.4-76.2 mm (1-3 in)) transducer was used. The bridge was indexed at 0.76 mm (0.030 in) per pass. The gain and the db were varied as necessary to produce the required C-Scan. The resultant C-Scan was a 1:1 plan view of the specimen.

C-Scans do not produce information about "defect" location through-the-thickness of the specimen. In order to get reliable C-Scan results it is preferable to have a "standard" panel, with known

defects, be scanned at the same time that the test panel is scanned. The Scan parameters are set to find the known defects in the "standard" panel and the test panel is scanned at the same setting. This procedure could not be used in this program because each combination would have required it's own standard due to thickness, volume-percent-fiber and matrix variations. In this program, each panel was scanned so that a piece of lead tape on one surface was shown in its actual size in the C-Scan. This standardized all the results to this one type of "defect".

Using this technique the following type of anomalies could be distinguished:

1. non-bonded areas,
2. missing fibers, or
3. out-of-alignment fibers.

In this program the results of the NDT were used (1) to avoid testing regions with obvious defects or, (2) where this could not be avoided to either remake or repress the panel or, (3) to aid in interpreting the test results.

APPENDIX B

APPENDIX B

PANEL LAY-OUT AND SPECIMEN GEOMETRIES

There were six basic specimen configurations used in this program but all were essentially rectilinear bars machined from the basic panel. Schematic diagrams of the test specimens are shown in Figures B-1 through B-6.

There were two basic panel sizes for each combination: 203 mm x 610 mm (8" x 24") and 203 mm x 229 mm (8" x 9"). All longitudinal tension, fatigue and shear specimens were taken from the 203 mm x 610 mm (8" x 24") panel. All transverse specimens were taken from the 203 mm x 229 mm (8" x 9") panel. Typical specimen lay-outs are shown in Figures B-7 and B-8. These lay-outs were modified when necessary to avoid anomalies shown by the NDT.

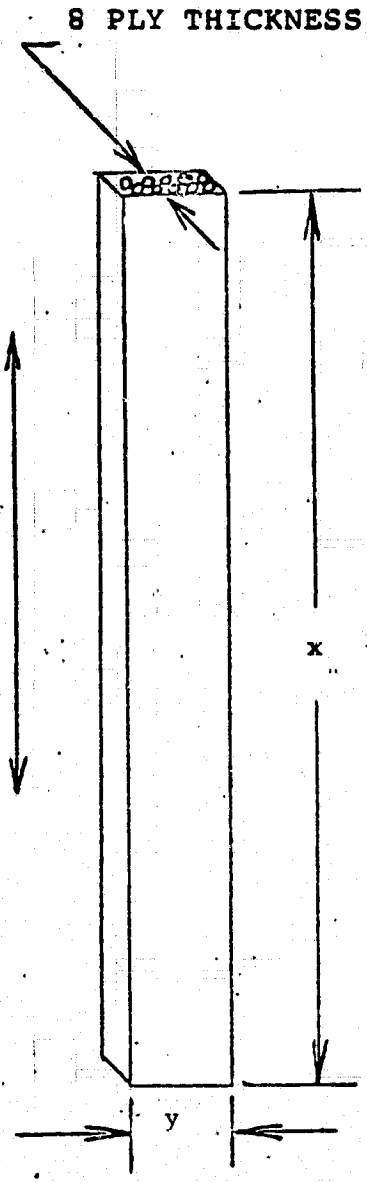

NOTE:

NOT DRAWN TO SCALE

x = 152 mm (6in) for room temperature

x = 229 mm (9in) for elevated temperature

y = 9.5 mm (0.375 in)

SPECIMEN CONFIGURATION FOR LONGITUDINAL TENSILE TESTS - ALL FILAMENT ORIENTATIONS

FIGURE B-1

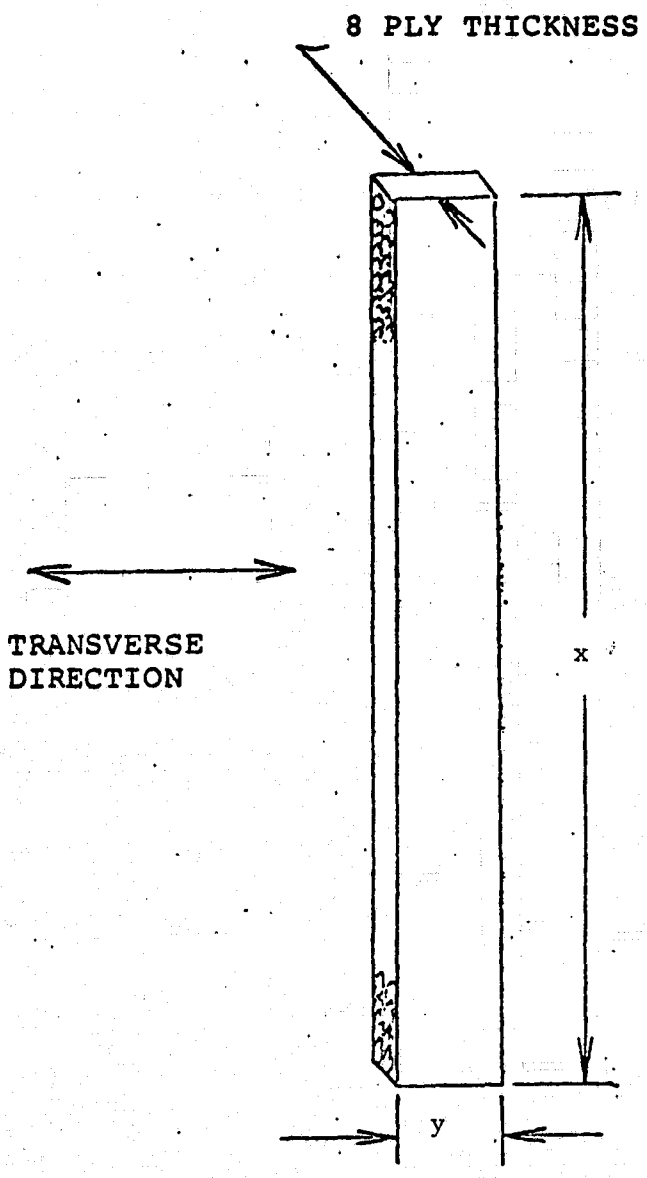

NOTE:

NOT DRAWN
TO SCALE

x = 152 mm (6 in) for room temperature
x = 229 mm (9 in) for elevated temperature
y = 9.5 mm (0.375 in)

SPECIMEN CONFIGURATION FOR TRANSVERSE TENSILE TESTS - ALL FILAMENT ORIENTATIONS

FIGURE B-2

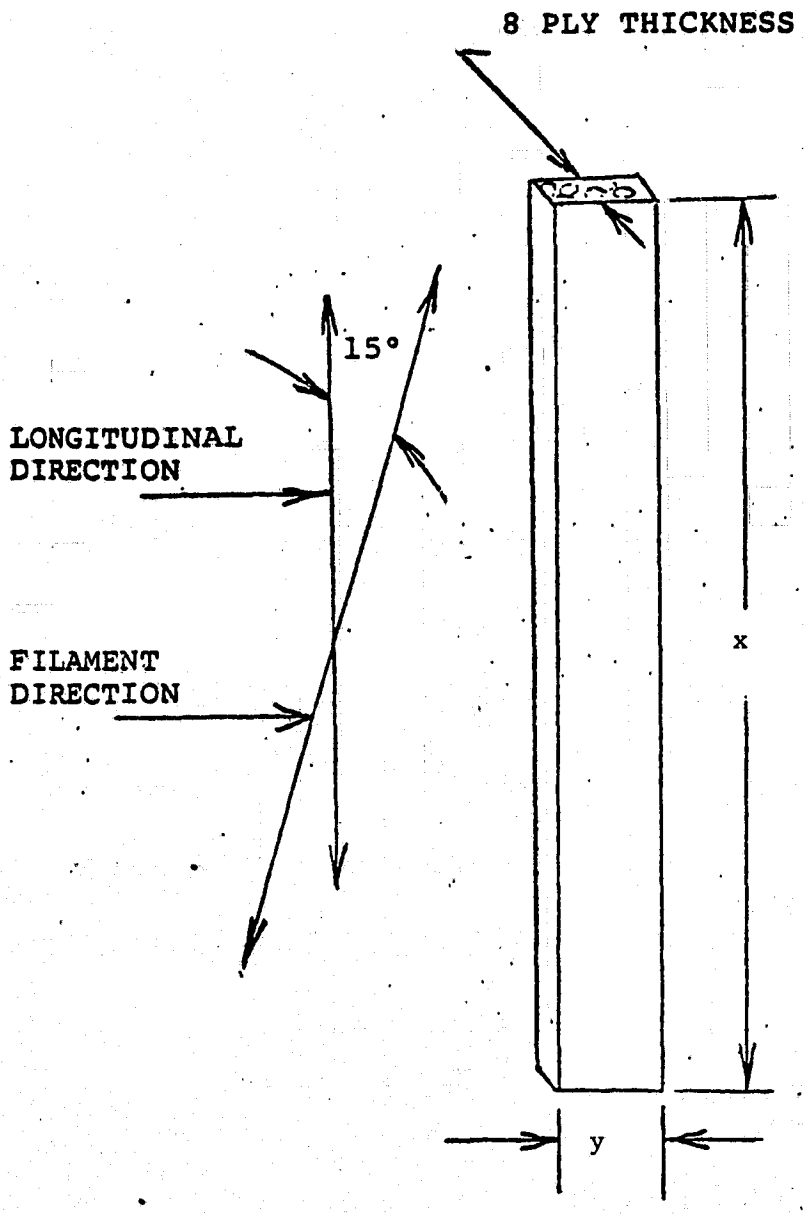

NOTE:

NOT DRAWN TO SCALE

x = 229 mm (9 in)
y = 12.7 mm (0.5 in)

SPECIMEN CONFIGURATION FOR LONGITUDINAL SHEAR TESTS OF 0° FILAMENT ORIENTATIONS ONLY

FIGURE B-3

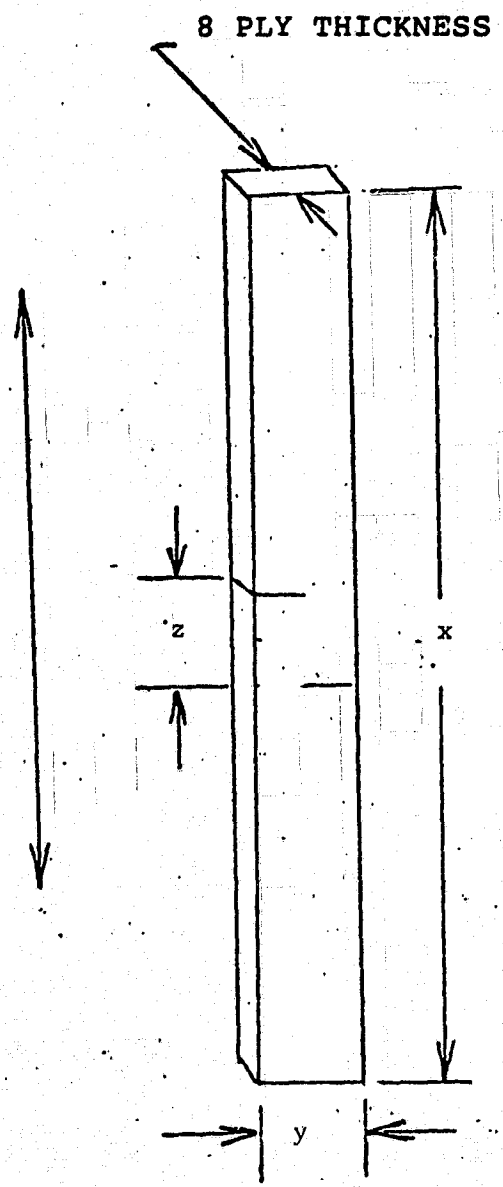

NOTE:
NOT DRAWN TO SCALE

x = 229 mm (9 in)
y = 12.7 mm (0.5 in)
z = 12.7 mm (0.5 in)

SPECIMEN CONFIGURATION FOR DOUBLE NOTCH SHEAR TESTS - ± FILAMENT ORIENTATIONS ONLY

FIGURE B-4

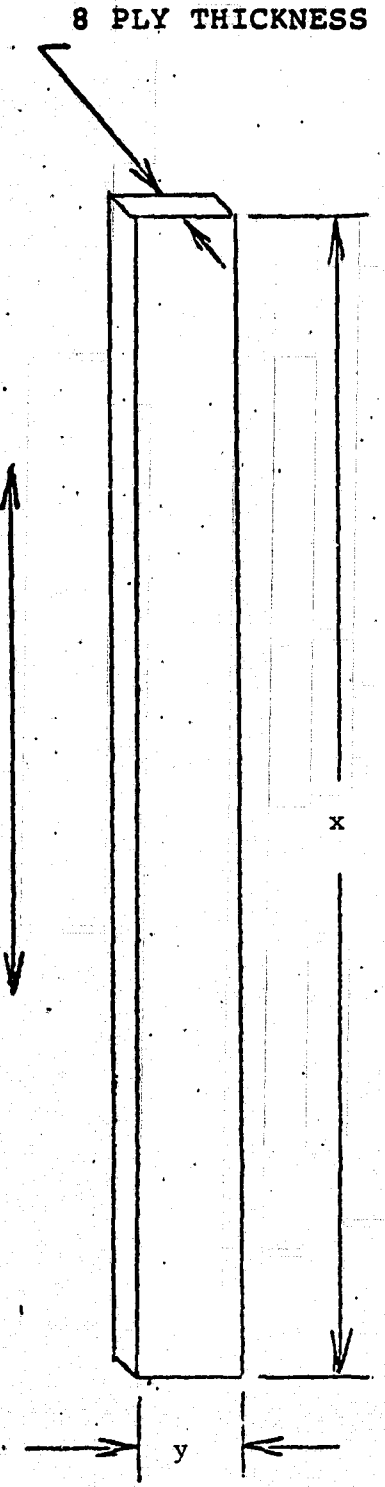

NOTE:
NOT DRAWN
TO SCALE

x = 610 mm (24 in) for elevated temperatures
x = 229 mm (9 in) for room temperatures
y = 12.7 mm (0.5 in)

SPECIMEN CONFIGURATION FOR LONGITUDINAL FATIGUE TESTS - ALL FILAMENT ORIENTATIONS

FIGURE B-5

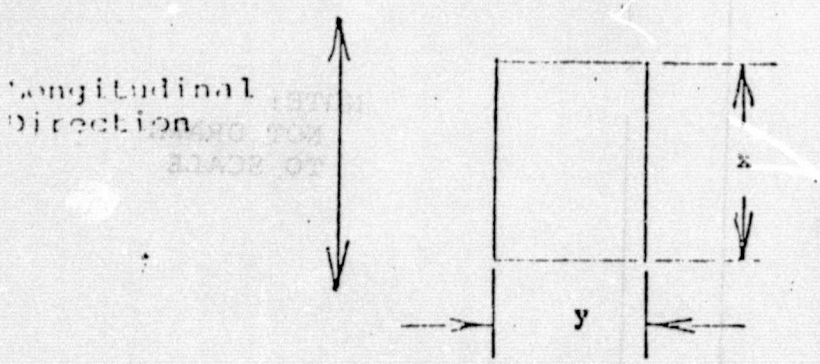

NOTE:

NOT DRAWN
TO SCALE

x = 7.1 mm (0.28 in)
y = 9.5 mm (0.375 in)

SPECIMEN CONFIGURATION
FOR THERMAL EXPANSION
TESTS - ALL FILAMENT
ORIENTATIONS

FIGURE B-6

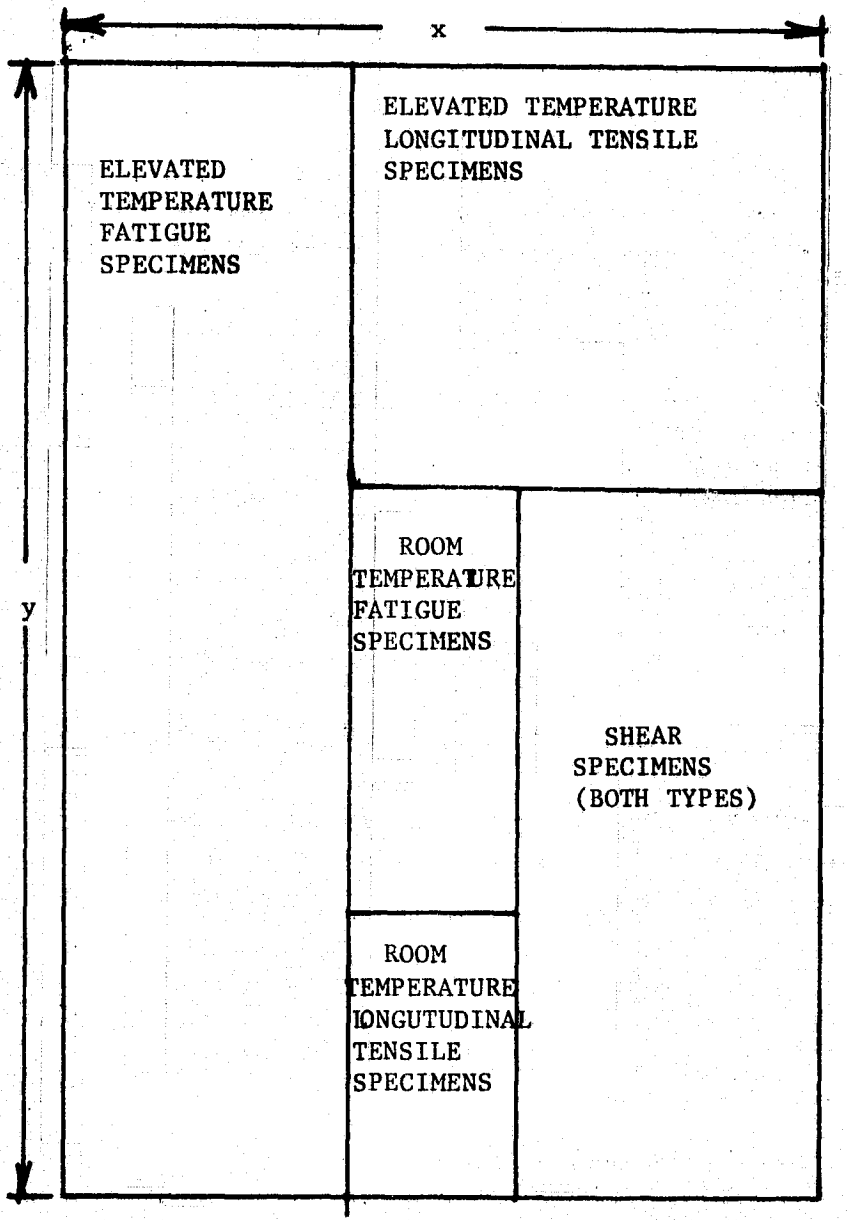

x = 203 mm (8 in) [1/2 scale]
y = 610 mm (24 in)[1/4 scale]
fiber direction

FIGURE B-7

TYPICAL SPECIMEN LAYOUT FOR LARGE PANELS

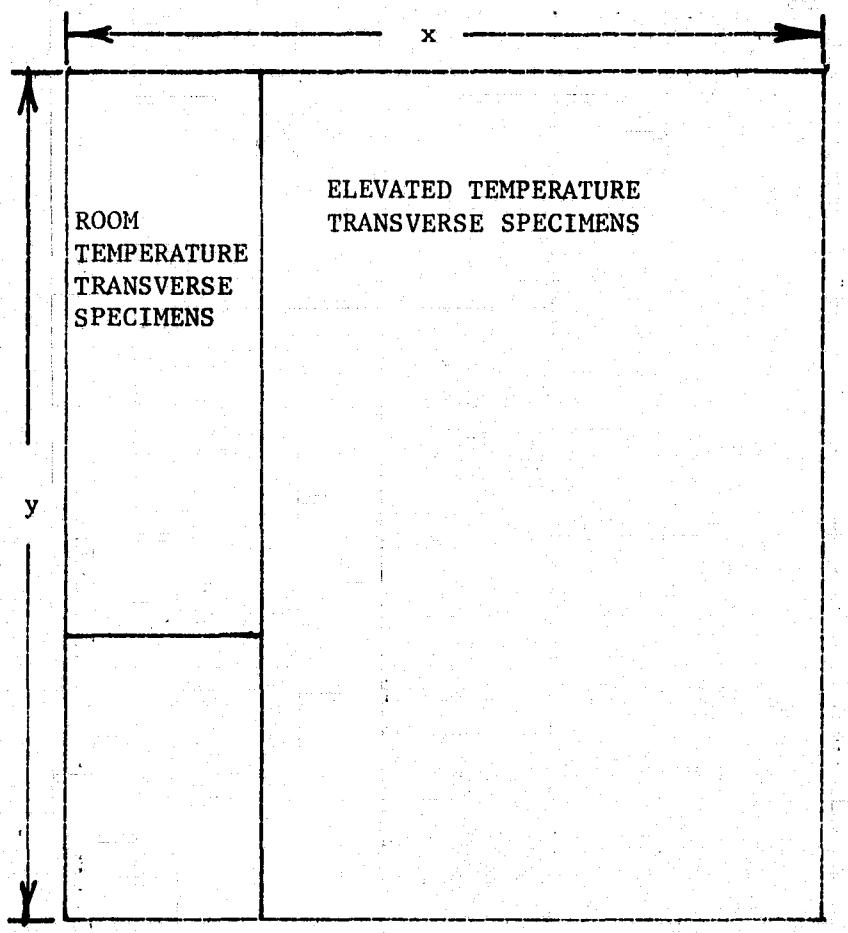

x = 203 mm (8 in) [i/2 scale]
fiber direction
y = 229 mm (9 in) [1/2 scale]

FIGURE B-8
TYPICAL SPECIMEN LAYOUT FOR SMALL PANELS

APPENDIX C

APPENDIX C

TEST PROCEDURES

Room Temperature Static Tests

Test specimens were strain gaged at the center line and tabbed with 51 mm (2 in) x 13 mm (0.5 in) 1100-0 Al tabs at the grip ends. Tests were run by the ramp-load method with a crosshead speed of 1.3 mm/min (0.05 in/min); strain readings were taken at 445 N (100 lb) load intervals at low load levels and at 2224 N (500 lb) load intervals at high load levels. The tests were run on an Instron Universal test machine using a 10,000 lb load cell. The strain measurements were made using a Vishay 220 Data Logging System. Strain gages were Micro Measurement 6 mm (1/4 in) long 0° gages.

Elevated Temperature Static Tests

Test specimens were tabbed with the same type of tabs as for RT tests except that a high temperature adhesive was used. Strain gages were applied as recommended by Micro Measurements for high temperature use. The specimens were heated as shown in the schematic (Figure C-1), using quartz lamp heating elements. Furnace temperature was controlled by a thermocouple placed at the inside top of the furnace via a Research Inc. controller. Specimen temperature was monitored by thermocouples placed just above specimen centerline on both surfaces of the specimen. Calibration

experiments showed that these temperatures were within ± 5°C of the temperature of the specimen interior.

During a test the specimens were placed in the furnace, lamps were turned on and the specimen was allowed to reach equilibrium at the desired temperature before test. In the case of 149°C tests the time required to reach temperature was ∿5 minutes; at 260°C the time was ∿10 minutes; at 371°C the time was ∿12 minutes. Tests at all temperatures required ∿10 minutes after the specimen had reached equilibrium temperature.

Shear Tests

For all 0° combinations a shear specimen was used which had the fibers oriented 15° off-axis to the tensile axis.[19] One of the principal motivations for the selection of this test specimen was the attempt to minimize the magnitude of the stress in the direction perpendicular to the fibers in order to avoid stress interaction effects in the determination of shear strength. In contrast, the transverse stress in a 45° off-axis test is equal in magnitude to the shear stress in the material principal directions. Thus, for the 45° case, it is possible that interaction effects may be significant. For the ± 15° combinations this type of specimen was not used because the fibers were already crossplied in the ± 15° direction and the test results would have been identical to the longitudinal tension tests for these materials. A double notch test, in common usage, was used instead for measurement of shear stress.

Fatigue and Thermal Expansion Tests

Test techniques for these tests are described in the body of the report.

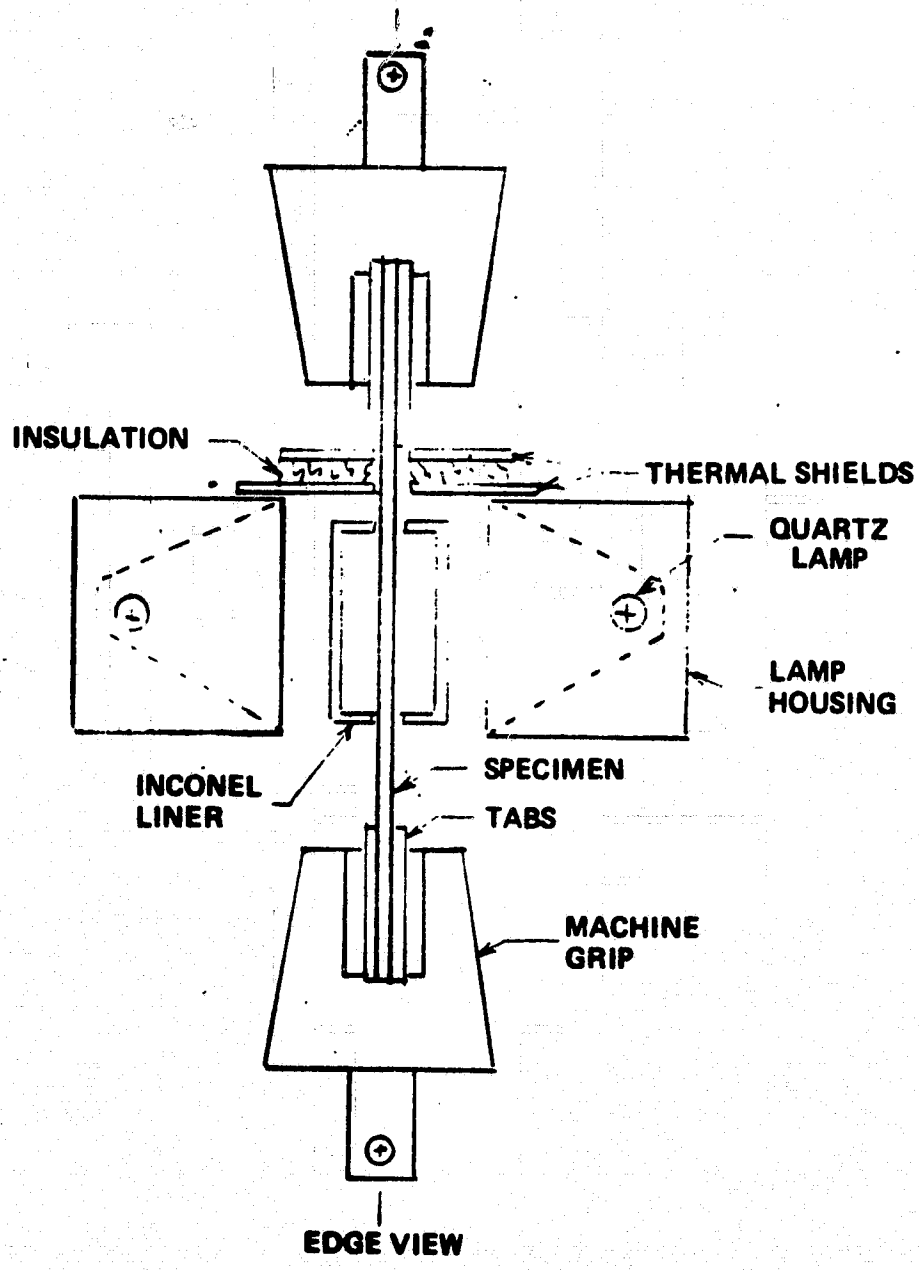

Figure C-1. Furnace Arrangement for Tensile Testing.

APPENDIX D

COMBINATION 1

Specimen	UTS (ksi)	E (Mpsi)	$\sigma_{15°}$ (ksi)	σ_B (ksi)
RTLT 1	201.8	27.2		
RTLT 2	205.3	27.2		
RTLT 3	197.2	27.2		
300 HTLT 1	216.5	25.5		
HTLT 2	196.8	25.0		
HTLT 4	177.8	24.0		
500 HTLT 6	178.9			
HTLT 8	184.7			
HTLT 9	116.6*			
700 HTLT 10	176.1			
HTLT 11	183.1			
RTTT 1	5.7	22.3		
RTTT 2	6.2	15.2		
RTTT 3	5.8	18.6		
300 HTTT 1	5.2	5.0		
HTTT 2	**			
HTTT 3	4.6			
500 HTTT 4	4.0			
HTTT 5	3.9			
HTTT 6	4.4			
SHEAR RTS			11.2	47.8
HTS 300°			9.9	39.5
HTS 500°			5.7	22.8***
HTS 500°			6.6	26.2****

* - not included in average

** - broke in handling

*** - no failure necked

**** - fracture net section tension

COMBINATION 2

Specimen	UTS (ksi)	E (Mpsi)	$\sigma_{15°}$ (ksi)	σ_B (ksi)
RTLT 3	167.3	25.1		
RTLT 4	167.2	25.3		
RTLT 5	191.6	25.2		
300 HTLT 11	182.0	25.7		
HTLT 12	170.3	26.0		
500 HTLT 9	177.0			
HTLT 10	198.7			
SHEAR RTS			12.45	49.8
HTS 300°			11.15	44.6
HTS 500°			9.2	36.7
HTS 500°			12.7	50.9

COMBINATION 3

Specimen	UTS (ksi)	E (Mpsi)	$\sigma_{15°}$ (ksi)	σ_B (ksi)
RTLF 1	240.0	35.0		
RTLF 2	247.0	34.9		
RTTT 1	7.4	20.7		
RTTT 2	9.8			
RTTT 3	7.0			
300 HTTT 1	7.8	24.4		
HTTT 2	7.0	17.5		
HTTT 3	6.2			
500 HTTT 4	5.6			
HTTT 5	4.5*			
HTTT 6	5.0			
SHEAR RTS			13.4	53.5
HTS 500°			12.4	49.7

* - broke before testing on heat up

COMBINATION 4

Specimen	UTS (ksi)	E (Mpsi)	$\sigma_{15°}$ (ksi)	σ_B (ksi)
RTLT 3	216.8	30.0		
RTLT 4	224.5	30.2		
RTLT 5	201.7			
300 HTLT 1	153.0	29.2		

COMBINATION 5

Specimen	UTS (ksi)	E (Mpsi)	$\sigma_{15°}$ (ksi)	σ_B (ksi)
RTLT 1	217.8	28.7		
RTLT 2	222.5	27.8		
RTLT 3	215.3	29.6		
300 HTLT 1	202.9	28.1		
HTLT 2	168.1	43.0*		
HTLT 3	226.6	31.4		
500 HTLT 4	212.5			
HTLT 5	189.5			
HTLT 6	209.5			
RTTT 1	12.6	24.3		
RTTT 2	12.0	19.8		
RTTT 3	11.3	24.1		
300 HTTT 1	9.5	34.1		
HTTT 2	8.5			
HTTT 3	7.6			
SHEAR RTS			11.1	47.2
HTS 500°			5.9	24.0

* - possible strain gage debond

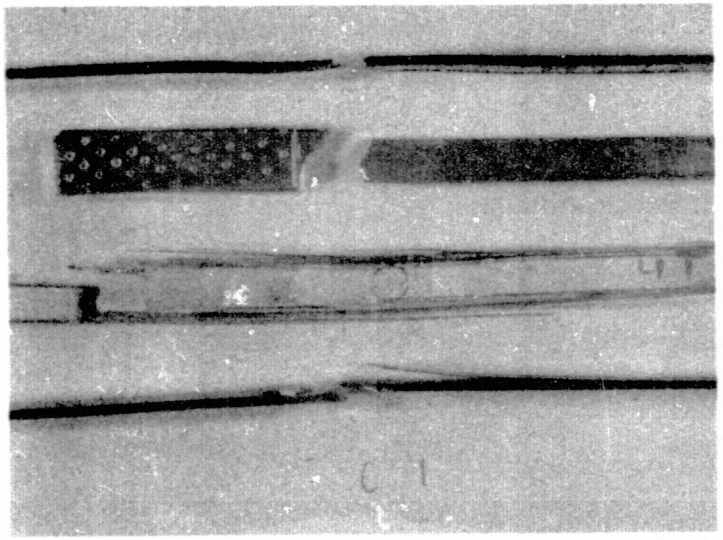

(a)

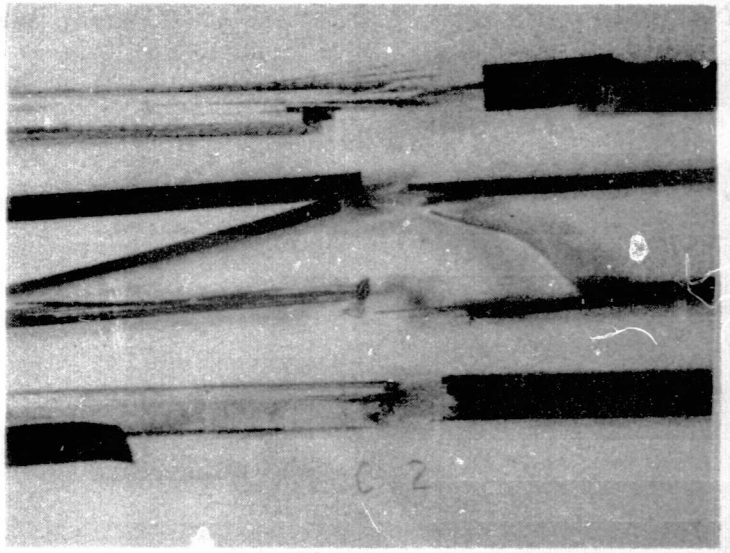

(b)

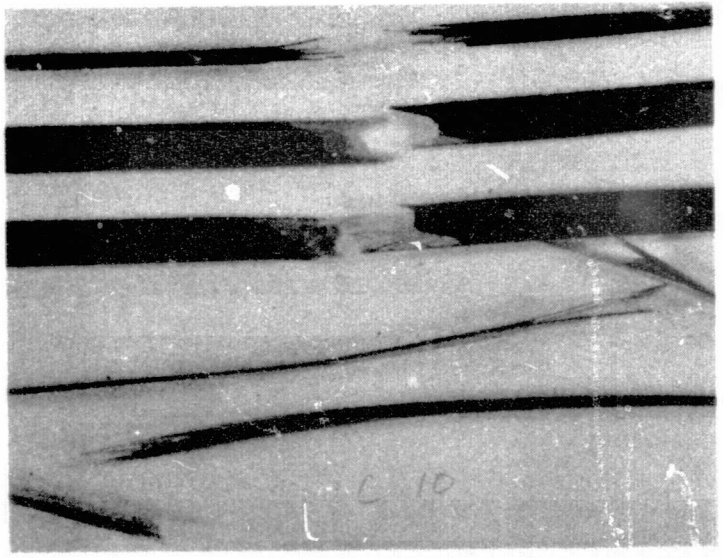

(c)

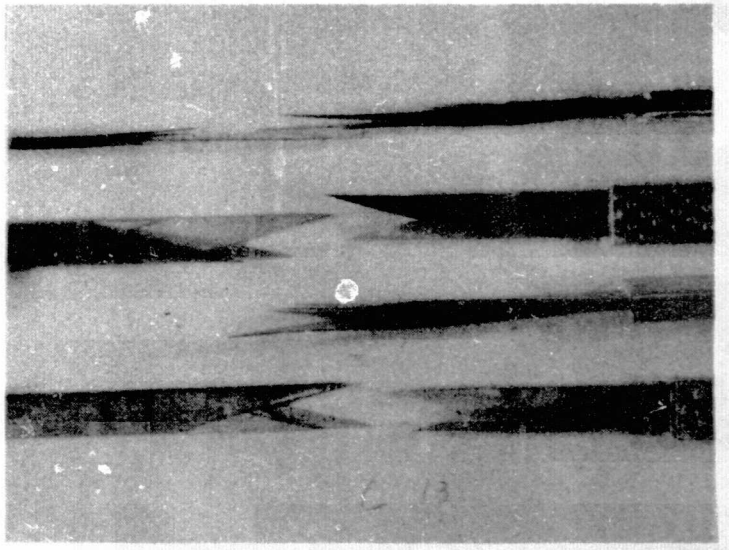

(d)

Figure II-11. Photographs of Failed 260°C (500°F) Fatigue Tests:

(a) Combination 1, (b) Combination 2, (c) Combination 10, and (d) Combination 13.

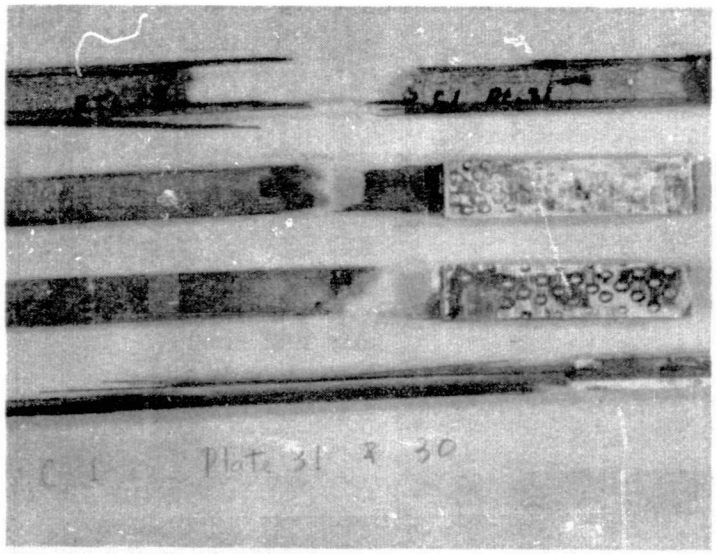

(a)

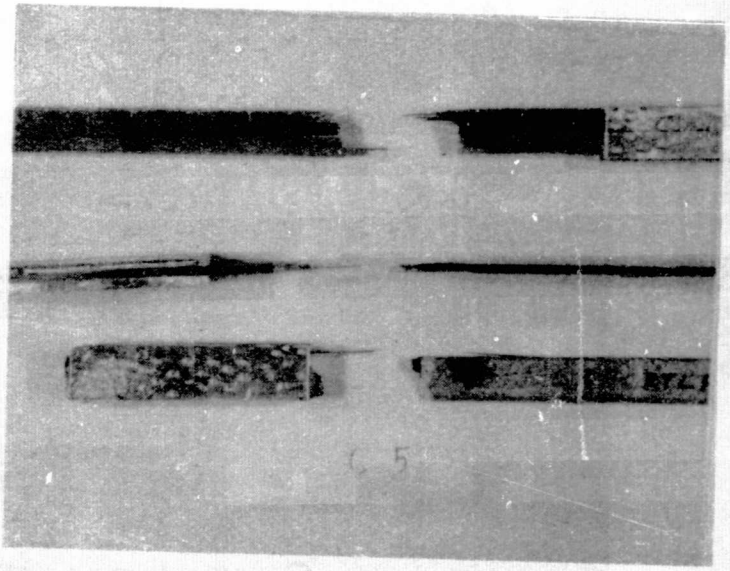

(b)

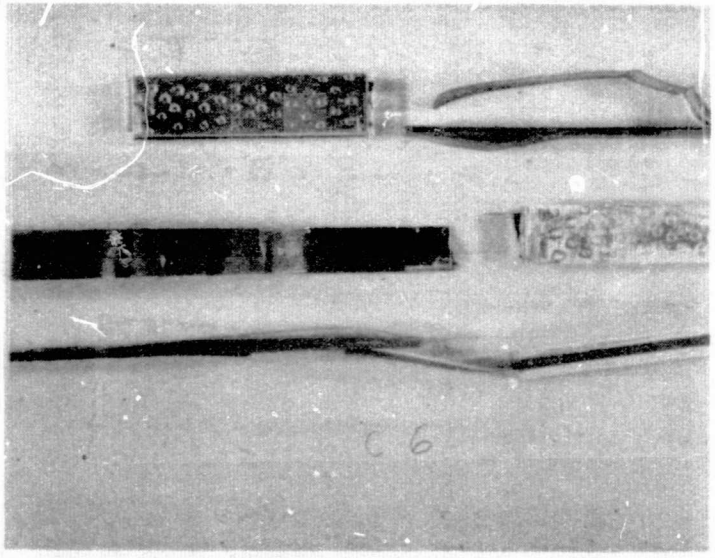

(c)

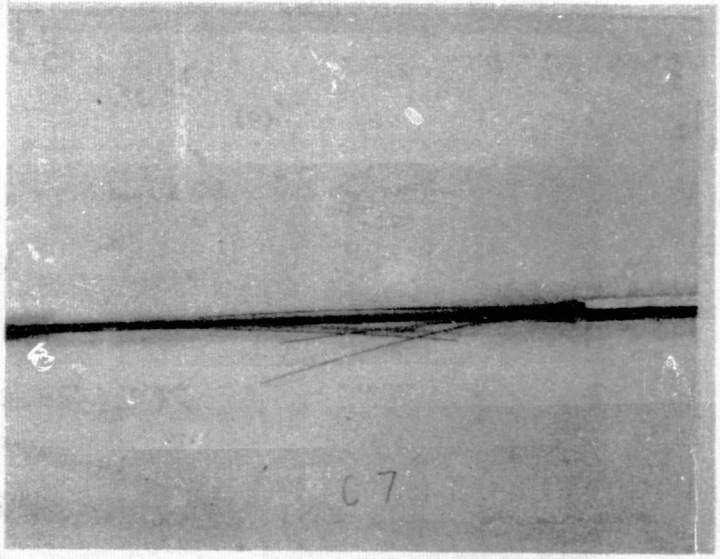

(d)

Figure II-12. Photographs of Failed Room Temperature Fatigue Tests:

(a) Combination 1, (b) Combination 5, (c) Combination 6, and (d) Combination 7.

COMBINATION 6

Specimen	UTS (ksi)	E (Mpsi)	$\sigma_{15°}$ (ksi)	σ_B (ksi)
RTLT 1	172.6	26.4		
RTLT 2	179.3	23.1		
RTLT 3	161.9			
300 HTLT 1	178.6	26.4		
HTLT 2	156.3	25.3		
HTLT 3	144.0			
500 HTLT 5	141.1			
HTLT 6	145.1			
HTLT 7	155.9			
SHEAR RTS			14.2	56.8

COMBINATION 7

Specimen	UTS (ksi)	E (Mpsi)	$\sigma_{15°}$ (ksi)	σ_B (ksi)
RTLT 1	218.0	30.8		
RTLT 2	232.1	30.1		
RTLT 3	182.8	34.5		
300 HTLT 1	193.8	*		
HTLT 2	211.9	30.5		
HTLT 3	214.0	*		
500 HTLT 4	169.1			
HTLT 5	206.0			
HTLT 6	193.9			
SHEAR RTS			5.5	23.4

* - gage failed

COMBINATION 8

Specimen	UTS (ksi)	E (Mpsi)	$\sigma_{15°}$ (ksi)	σ_B (ksi)
RTLT 1	159.0	32.9		
RTLT 2	119.1	32.3		
RTLT 3	152.7	31.5		
300 HTLT 1	203.2	29.4		
HTLT 2	213.4	29.5		
HTLT 3	213.9			
500 HTLT 4	228.6			
HTLT 5	201.0			
HTLT 6	224.6			
RTTT 1	30.3			
RTTT 2	30.3	20.4		
RTTT 3	30.0			
300 HTTT 1	24.8	7.1		
HTTT 2	22.9	5.9		
HTTT 3	20.1			
500 HTTT 4	19.8	5.5		
HTTT 5	19.8			
HTTT 6	20.0			
SHEAR HTS 300°			10.1	40.5
HTS 500°			10.6	42.4

COMBINATION 9

Specimen	UTS (ksi)	E (Mpsi)	$\sigma_{15°}$ (ksi)	σ_B (ksi)
RTLT 1	151.0	30.4		
RTLT 2	153.0			
RTLT 3	141.6			
300 HTLT 1	157.0			
HTLT 2	139.4	22.0		
HTLT 3	126.2			
500 HTLT 4	109.1			
HTLT 5	111.6			
RTTT 1	14.5			
RTTT 2	15.4			
RTTT 3	13.9			
300 HTTT 1	10.5	5.6*		
HTTT 2	9.4	4.7*		
HTTT 3	9.2			
500 HTTT 4	7.5	3.0*		
HTTT 12	6.8			
SHEAR RTS				24.1
RTS				14.6
HTS 700°				12.3

* - initial

COMBINATION 10

Specimen	UTS (ksi)	E (Mpsi)	$\sigma_{15°}$ (ksi)	σ_B (ksi)
RTLT 1	72.0	*		
RTLT 2	61.2	*		
300 HTLT 10	133.4	24.7		
HTLT 11	129.3			
HTLT 12	115.6			
300 HTTT 1	26.7			
HTTT 2	22.8			
500 HTTT 4	15.6			
SHEAR RTS				>20.4
HTS				>21.1

* - debond

COMBINATION 10

(REMADE)

Specimen	UTS (ksi)	E (Mpsi)	$\sigma_{15°}$ (ksi)	σ_B (ksi)
RTLT 1	125.1	22.6		
RTLT 2	153.3	30.2		
RTLT 3	143.9	20.1		
300 HTLT 1	109.9	17.4		
HTLT 2	114.2			
500 HTLT 4	113.3			
HTLT 5	105.8			
700 HTLT 7	83.0			
HTLT 8	84.6			
HTLT 9	88.7			
RTTT 1	22.7	13.8		
RTTT 2	26.7	18.3		
RTTT 3	25.8			
RTTT 4	23.2			
300 HTTT 1	21.1			
HTTT 2	22.4	9.9		
HTTT 3	15.6			
HTTT 10	18.2	13.8		
500 HTTT 4	17.6			
HTTT 5	17.6			
HTTT 6	16.3			
HTTT 7	15.4	6.2		
SHEAR HTS 500°				>16.4
HTS 500°				>17.4

COMBINATION 11

Specimen	UTS (ksi)	E (Mpsi)	$\sigma_{15°}$ (ksi)	σ_B (ksi)
RTLT 1	103.4	35.6		
RTLT 2	90.3	37.4		
RTLT 3	96.6			
300 HTLT 1	148.3			
HTLT 2	163.6	25.4		
500 HTLT 4	143.5			
HTLT 5	*			
RTTT 1	15.8	35.7		
RTTT 2	13.3			
RTTT 3	12.7			
300 HTTT 6	8.0			
HTTT 4	8.3	7.7		
HTTT 5	8.3	8.8		
500 HTTT 9	5.9			
HTTT 8	6.4			
HTTT 7	6.8	1.7*		
SHEAR RTS				24.4
HTS				24.6

* - initial

COMBINATION 12

Specimen	UTS (ksi)	E (Mpsi)	$\sigma_{15°}$ (ksi)	σ_B (ksi)
RTLT 1	165.1	25.1		
RTLT 2	155.1	29.7		
RTLT 3	144.1			
300 HTLT 1	173.8	26.4		
HTLT 2	144.9	30.4		
HTLT 3	174.6			
500 HTLT 4	142.9			
HTLT 5	141.3			
HTLT 6	133.1			
SHEAR RTS				>21.8
HTS				>24.5

COMBINATION 13

Specimen	UTS (ksi)	E (Mpsi)	$\sigma_{15°}$ (ksi)	σ_B (ksi)
RTLT 1	152.3	26.3		
RTLT 2	146.5	25.5		
RTLT 3	66.1**			
300 HTLT 1	138.7	25.4		
HTLT 2	130.9	24.9		
HTLT 3	140.2			
500 HTLT 4	127.8			
HTLT 5	144.8			
HTLT 6	106.4			
RTTT 1	20.5	*		
300 HTTT 1	15.7	*		
HTTT 2	10.8			
500 HTTT 4	9.1			
HTTT 5	6.8			
SHEAR RTS				>17.2
HTS 300°				>17.6
HTS 500°				>16.7
HTS 500°				>16.5

* - strain readings erratic

** - specimen defective

COMBINATION 14

Specimen	UTS (ksi)	E (Mpsi)	$\sigma_{15°}$ (ksi)	σ_B (ksi)
RTLT 1	150.5	28.7		
RTLT 2	177.8	28.2		
RTLT 3	155.3			
300 HTLT 1	149.8	26.3		
HTLT 2	*			
HTLT 3	171.6			
500 HTLT 4	*			
HTLT 5	160.0			
HTLT 6	*			
RTTT 1	16.5			
RTTT 2	15.3			
RTTT 3	13.5			
300 HTTT 4	9.9			
HTTT 6	9.8			
500 HTTT 7	6.6			
HTTT 8	6.6			
HTTT 9	7.4			
SHEAR HTS 300°				>14.5

* - debonded before test

C-2

COMBINATION 15

Specimen	UTS (ksi)	E (Mpsi)	$\sigma_{15°}$ (ksi)	σ_B (ksi)
RTLT 1	119.2			
RTLT 2	169.0	32.2		
RTLT 3	155.7			
300 HTLT 1	164.8			
HTLT 2	195.3	33.0		
500 HTLT 4	130.9			
HTLT 5	111.6			
RTTT 1	15.2	34.0*		
RTTT 2	15.9			
RTTT 3	9.97			
300 HTTT 1	13.8	16.5*		
HTTT 2	13.2	21.6*		
HTTT 3	7.9			
500 HTTT 4	12.3	39.1*		
HTTT 5	8.8			
HTTT 6	11.7			
SHEAR RTS				25.4
HTS 300°				32.2
HTS 500°				29.5

* - initial

COMBINATION 16

Specimen	UTS (ksi)	E (Mpsi)	$\sigma_{15°}$ (ksi)	σ_B (ksi)
RTLT 1	36.1	27.1		
RTLT 2	40.9	28.5		
RTLT 3	40.9			
300 HTLT 1	36.0	23.0		
HTLT 2	37.6	22.9		
HTLT 3	30.9			
500 HTLT 4	29.3			
HTLT 5	28.9			
HTLT 6	32.0			
RTTT 1	20.1	23.9*		
RTTT 2	20.0	20.8*		
RTTT 3	23.1	15.3*		
300 HTTT 1	19.4	20.8		
HTTT 2	22.8	23.8*		
HTTT 3	22.9			
500 HTTT 4	14.6	11.6*		
HTTT 5	22.1			
HTTT 6	15.9			
SHEAR RTS				>11.0
HTS 300°				> 8.4
HTS 500°				> 6.3

* - initial

COMBINATION 17

Specimen	UTS (ksi)	E (Mpsi)	$\sigma_{15°}$ (ksi)	σ_B (ksi)
RTLT 1	50.0	23.1		
RTLT 2	67.4	27.0*		
300 HTLT 1	61.6	26.7		
HTLT 2	52.4	25.2		
HTLT 3	60.0			
500 HTLT 4	26.2			
HTLT 5	79.6			
HTLT 6	47.3			
RTTT 1	15.0	36.4*		
RTTT 2	17.4			
RTTT 3	21.6	13.4		
300 HTTT 4	16.9	21.8**		
HTTT 5	18.6	15.2*		
HTTT 6	20.5			
500 HTTT 7	16.5	21.6**		
HTTT 8	12.8			
HTTT 9	16.8			
SHEAR RTS				>10.3
HTS 500°				> 9.7

* - straight line slope

** - initial

APPENDIX E

Appendix E
Parametric Study

Introduction

Because difficulties were encountered in gripping tensile specimens efficiently when specimen breaking loads exceeded 6000 lbs, NETCO undertook an internally funded parametric study of test techniques with the primary objectives being the identification of 1) the best tab material, 2) the minimum grip length necessary to provide a positive grip during test, 3) the adhesive system which would best bond the tab to the specimen and 4) the width of the specimen to provide consistent and reliable results. During this study, the following test specimen parameters (shown in Figure 1) were investigated:

- Grip length (L_1)
- Gage width (W_2)
- Specimen thickness (t)
- Adhesive type

Approach

The conventional test specimen for oriented composite materials is straight sided, i.e., the grip width is equal to the gage width. The parametric study used straight sided specimens in which the gage width was varied from 3.175 mm (0.125 in) to 12.7 mm (0.5 in).

The overall length of the test specimen was held constant at 152 mm (6 in).

Specimen grip length was varied from 38.1 mm (1.5 in) to 50.8 mm (2.0 in). The majority of the test specimens had a thickness of eight layers, since this material is of most interest to NASA. However, specimens consisting of 3 layers were also included in order to study the effect of specimen thickness.

The adhesive used to bond the tab to the specimen must have a shear strength capable of withstanding at least 5000 psi. The adhesives investigated in this study were 1) Miller Stephenson 907 epoxy, 2) Armstrong A12 epoxy and 3) M-Bond adhesive obtained from Micro Measurements. (This adhesive is similar to Eastman 910.) All specimen tabs consisted of 2.286 mm (0.090 in) thick 1100 Al in the dead soft condition.

The fiber used to make the test material was chosen to be 8 mil B/W because, for any given number of layers, these will produce the thickest specimen and therefore the highest breaking loads. The matrix was chosen to be 6061 Al because this produces the highest and most consistent ultimate strength composites and therefore requires the highest breaking loads.

The purpose of test matrix 1 was to determine which adhesive(s) and grip length (L_1) is most effective in testing these composites.

Test matrix 2 used the results obtained from test matrix 1 to determine which gage width(s) (W_2) produced the most consistent test results.

Results and Discussion of Results

Effect of Tab Grip Length

Figure 2 shows the results of the tests outlined in test matrix 1. Using tabs 38.1 mm (1.5 in) long, only the Armstrong A12 epoxy held the tabs on the specimens to failure. Using tabs 50.8 mm (2.0 in) long, all the adhesive systems held the tabs on to failure, even to maximum loads in excess of 44.5 kN (10,000 lbs).

Based upon these test results all the specimens in test matrix 2 were tabbed with 2.0 inch long 1100 Al in the dead soft condition using M-Bond adhesive. A total of 24 tests were performed. Twelve were done on 8 layer B/Al. Of these, nine broke in the gage length section, two broke in the tabbed section and one slipped. Twelve were done on 3 layer B/Al. Of these, six broke in the gage length and six broke in the tabbed section. There were no adhesive failures for this group.

From an analysis of our data it appears that, for 8 layer B/Al, the ultimate strength of the composite is not affected by gage widths 6.35 mm (0.25 in) or greater, up to the maximum width tested, 12.7 mm (0.5 in). However, 3 layer B/Al composites show a continuous increase in ultimate strength as gage width increased from 3.175 mm (0.125 in) to 12.7 mm (0.5 in).

Based on the results of this study, it is recommended that specimen width be 9.525 mm (0.375 in) for all 8 layer composites and that tabs be used which are 50.8 mm (2 in) long and made of 1100 Al in the dead soft condition. Any of the adhesives used on this study will work at the 2 inch grip length.

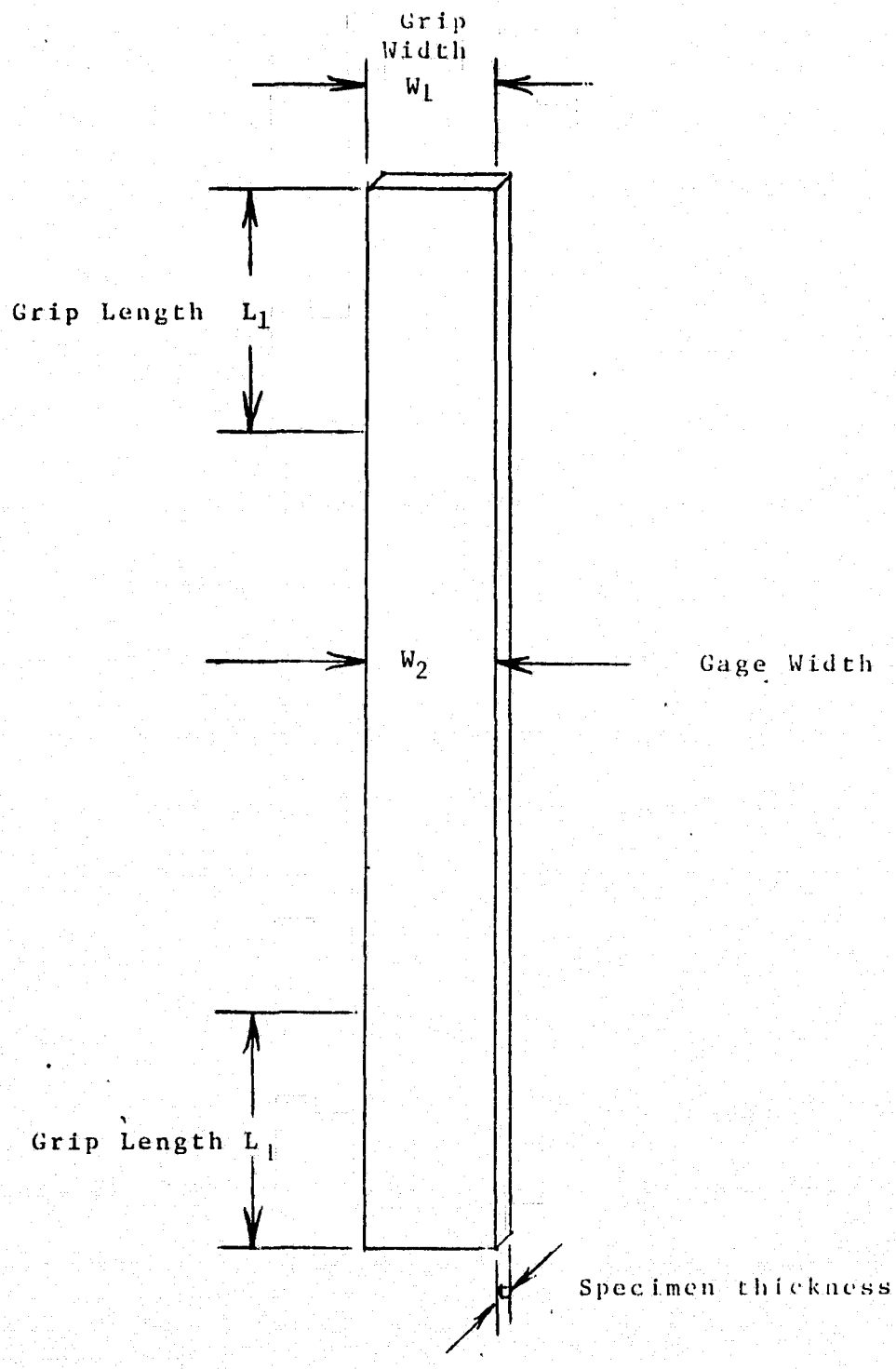

SCHEMATIC OF TEST SPECIMEN

FIGURE E-1

Test Matrix 1.

Variables: adhesive and grip length

	ADHESIVE		
Grip Length	M Bond	MS907	Armstrong \12
38.1 mm (1.5 in)	2 tests	2 tests	2 tests
50.8 mm (2.0 in)	3 tests	3 tests	3 tests

Test Matrix 2.

Variables: specimen width (W_2) and material thickness (t).

MATERIAL	SPECIMEN WIDTH (W_2)			
	3.175 mm (0.125 in)	6.350 mm (0.250 in)	9.525mm (0.375 in)	12.70 mm (0.50 in)
8 mil B/W/6061 Al t = 8 layer	3 tests	3 tests	3 tests	3 tests
t = 3 layer	3 tests	3 tests	3 tests	3 tests

Specimen Dimensions: 152 mm (6 in) long x X wide x X thick.

GRIP LENGTH (l_1), GRIP ADHESIVE STUDY

TEST MATRIX 1

PANEL 2b
MATERIAL: 8 mil B/W, 6061 Al, 8 layer
SPECIMEN DIMENSIONS: 152.4 mm X 9.5 mm (6 in X 0.375 in)

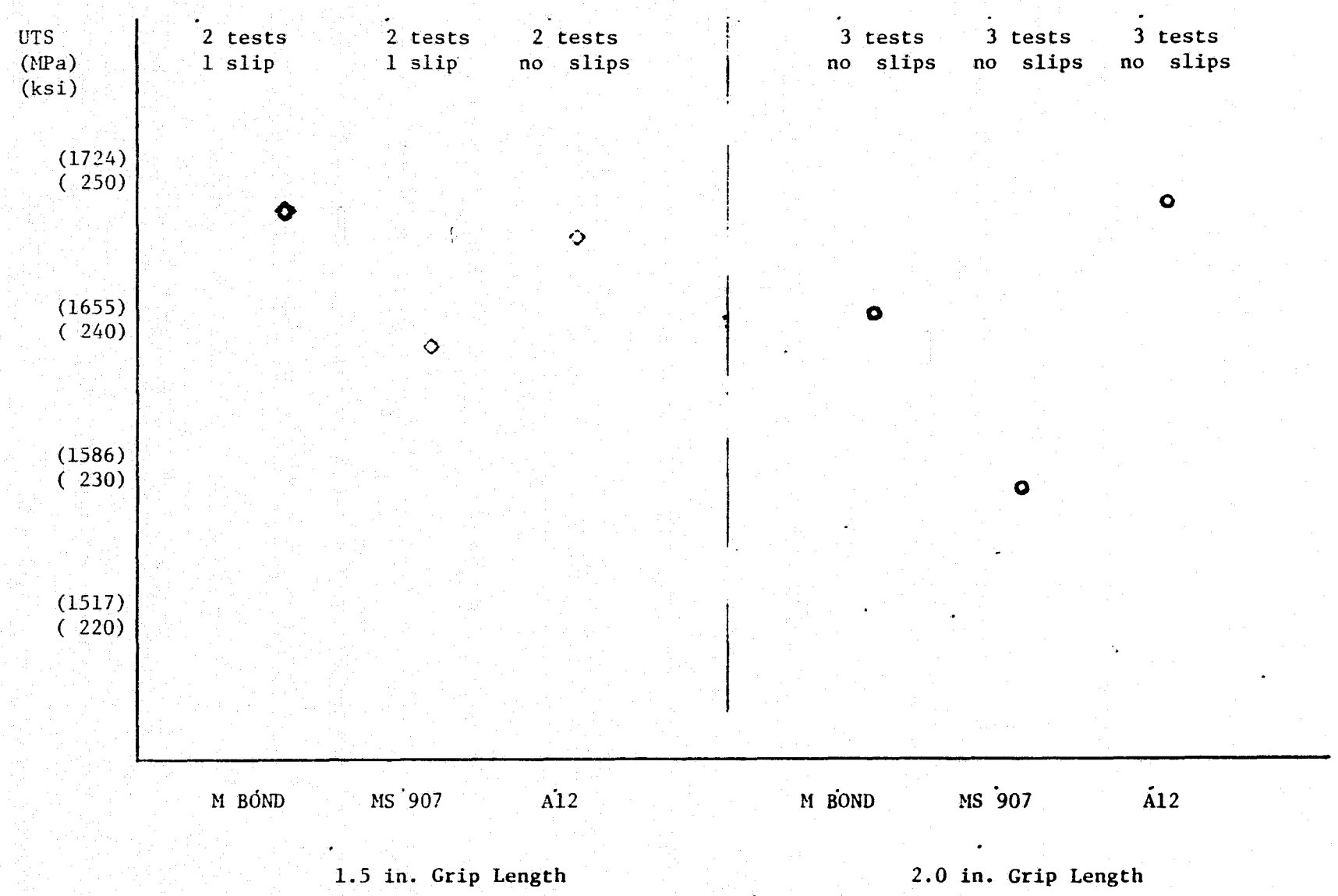

FIGURE 2.

APPENDIX F

APPENDIX F

NDT OF DELIVERABLE PANELS

The deliverable panels were NDT'd by the C-Scan technique described in Appendix B with the exception that both surfaces were Scanned instead of only one. This technique of scanning from both sides occasionally provides information on the near surface "grey" area which might be missed.

The C-Scans showed that the panels were generally well bonded with the exception of a very few anomalous areas. From past experience these areas shown in Figures F-1,F-2,F-3 & F-4, can be related to a missing, or slightly skewed, fiber somewhere in the 8 layers. They do not generally affect performance adversely when so few areas are involved.

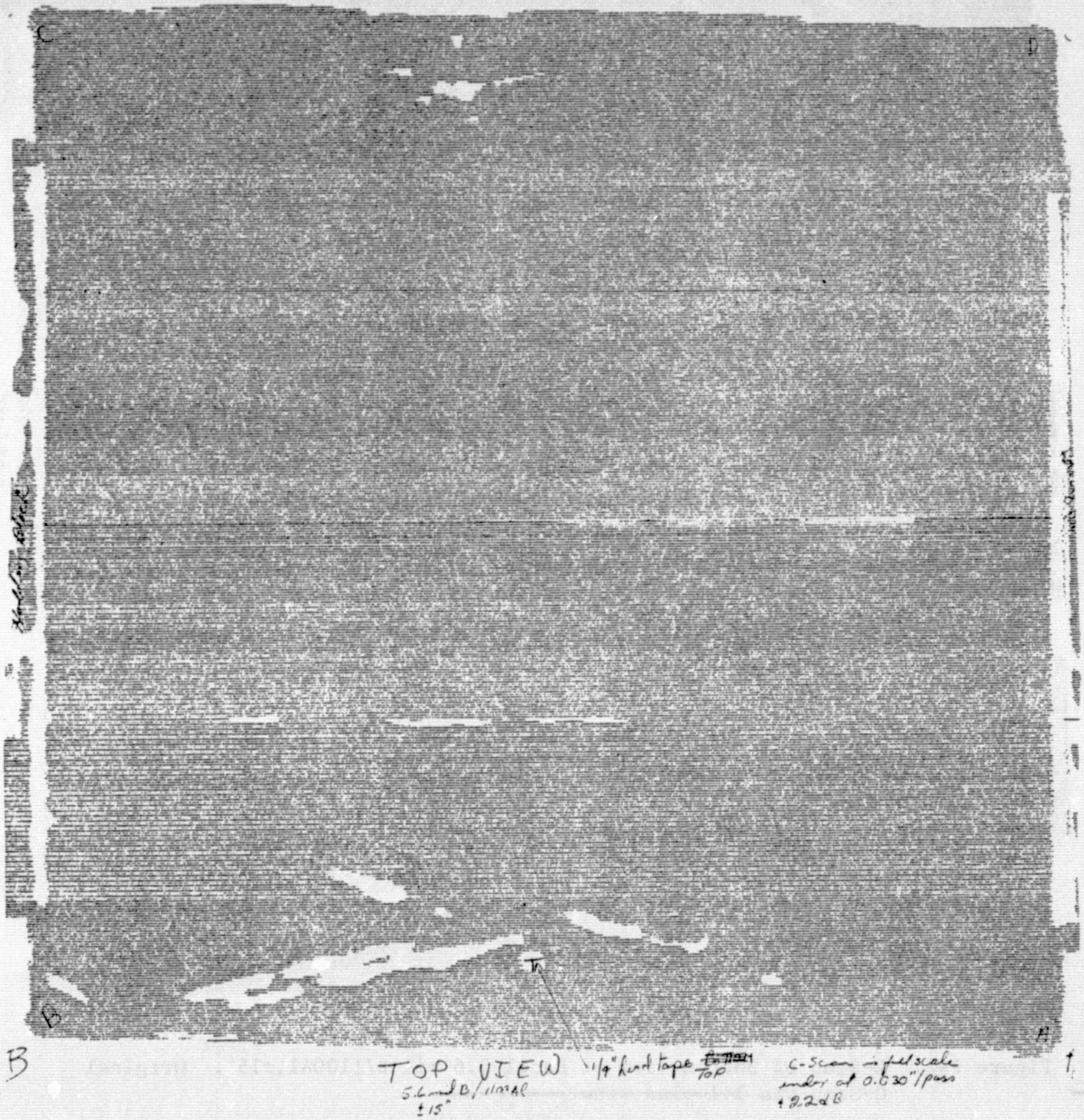

Figure F-1. C-Scan of top view of Panel 5.6 mil B/1100A1,±15°.
Original C-Scan was 1:1 plan view

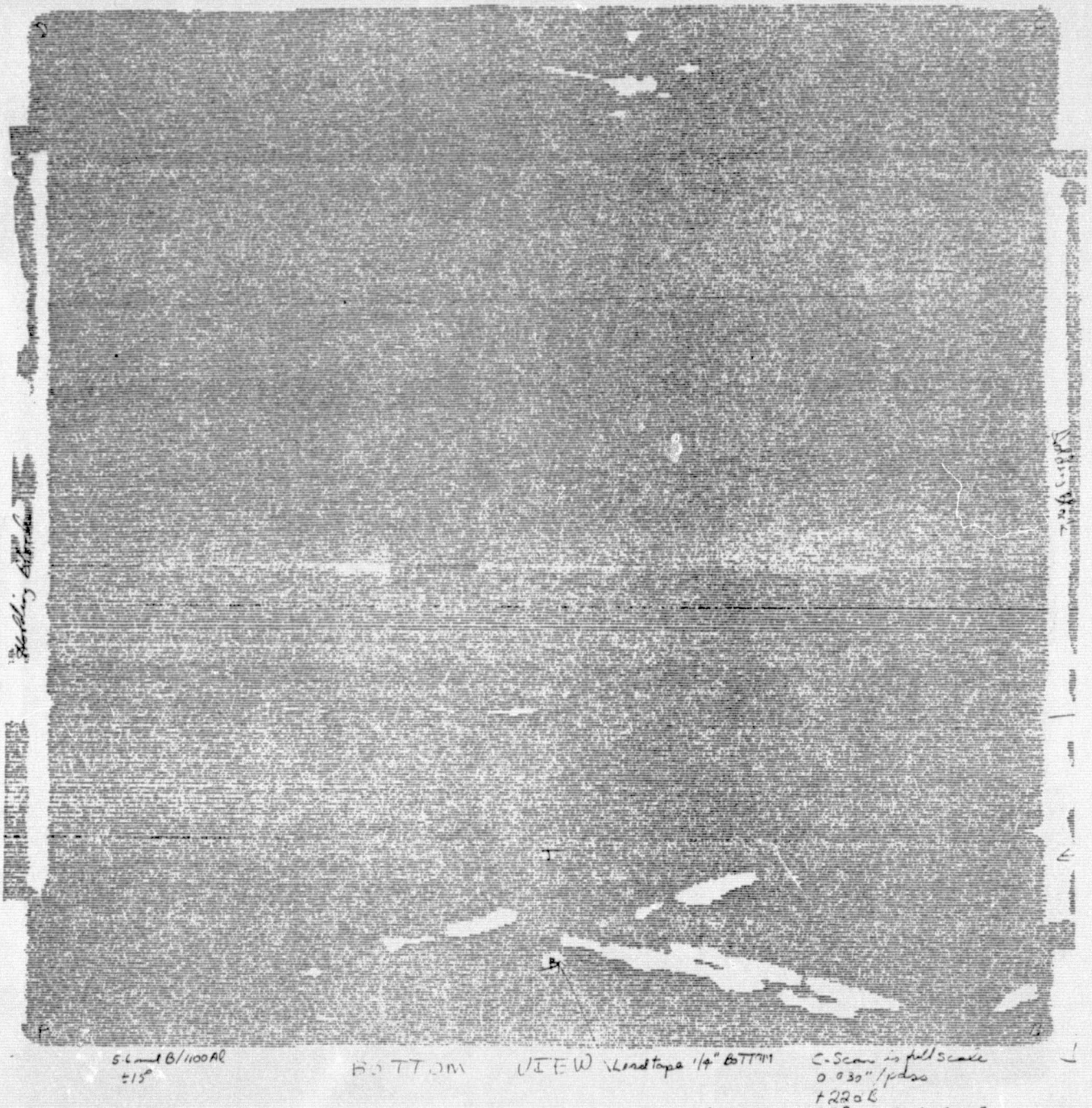

Figure F-2. C-Scan of Bottom view of Panel 5.6 mil B/1100Al,±15°. Original C-Scan was ~~1:1 plan view.~~

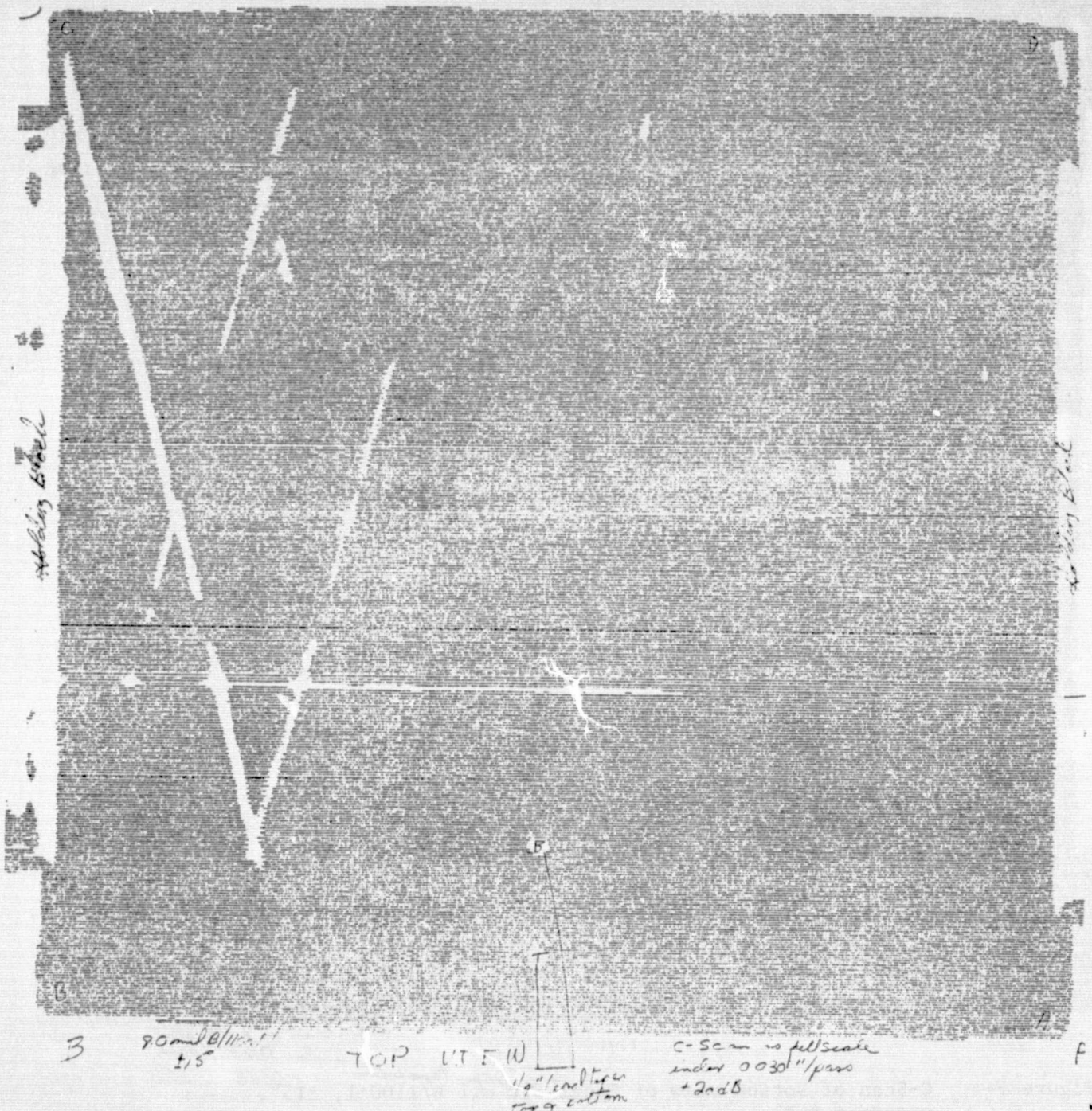

Figure F-3. C-Scan of Top view of Panel 8.0 mil B/1100Al, ±15°. Original C-Scan was 1:1 plan view.

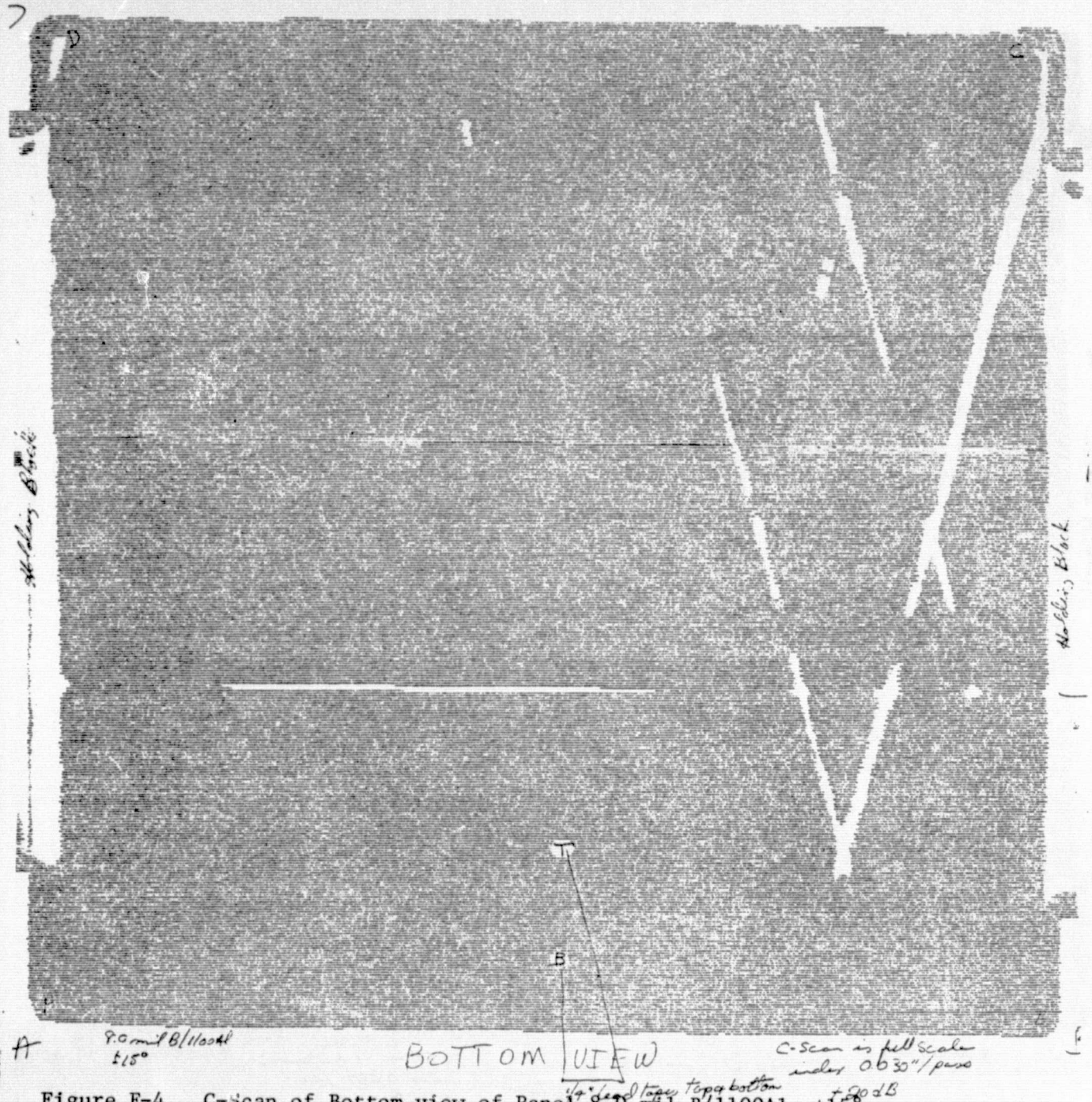

Figure F-4. C-Scan of Bottom view of Panel 8.0 mil B/1100A1, ±15°. Original C-Scan was 1:1 plan view.